



# Emerging ultrafast nucleic acid amplification technologies for next-generation molecular diagnostics

Sang Hun Lee<sup>a</sup>, Seung-min Park<sup>b</sup>, Brian N. Kim<sup>c</sup>, Oh Seok Kwon<sup>d</sup>, Won-Yep Rho<sup>e</sup>, Bong-Hyun Jun<sup>f,\*</sup>

<sup>a</sup> Department of Bioengineering, University of California Berkeley, CA, USA

<sup>b</sup> Department of Radiology, Stanford University, CA, USA

<sup>c</sup> Department of Electrical and Computer Engineering, University of Central Florida, FL, USA

<sup>d</sup> Infectious Disease Research Center, Korea Research Institute of Bioscience & Biotechnology, Daejeon, South Korea

<sup>e</sup> School of International Engineering and Science, Chonbuk National University, Jeonju, South Korea

<sup>f</sup> Department of Bioscience and Biotechnology, Konkuk University, South Korea

## ARTICLE INFO

### Keywords:

Nucleic acid amplification test  
Ultrafast polymerase chain reaction  
Isothermal amplification  
Point-of-care testing  
Artificial intelligence

## ABSTRACT

Over the last decade, nucleic acid amplification tests (NAATs) including polymerase chain reaction (PCR) were an indispensable methodology for diagnosing cancers, viral and bacterial infections owing to their high sensitivity and specificity. Because the NAATs can recognize and discriminate even a few copies of nucleic acid (NA) and species-specific NA sequences, NAATs have become the gold standard in a wide range of applications. However, limitations of NAAT approaches have recently become more apparent by reason of their lengthy run time, large reaction volume, and complex protocol. To meet the current demands of clinicians and biomedical researchers, new NAATs have developed to achieve ultrafast sample-to-answer protocols for the point-of-care testing (POCT). In this review, ultrafast NA-POCT platforms are discussed, outlining their NA amplification principles as well as delineating recent advances in ultrafast NAAT applications. The main focus is to provide an overview of NA-POCT platforms in regard to sample preparation of NA, NA amplification, NA detection process, interpretation of the analysis, and evaluation of the platform design. Increasing importance will be given to innovative, ultrafast amplification methods and tools which incorporate artificial intelligence (AI)-associated data analysis processes and mobile-healthcare networks. The future prospects of NA POCT platforms are promising as they allow absolute quantitation of NA in individuals which is essential to precision medicine.

## 1. Introduction

Innovative biotechnologies that integrate molecular biology, microfabrication and platform technologies are ushering new diagnostic tools toward next-generation disease detection (Hahm et al., 2018; Lee et al., 2012a; Liong et al., 2013; Park et al. 2016, 2017). The innovations and technological advances of the next-generation diagnostics in the academic fields are now well primed to appear in the industrial sectors (Lee et al., 2012b). For instance, the diagnostic company 'Theranos,' founded by Elizabeth Holmes, galvanized excitement about the potential in next-generation diagnostics, proposing the concept of detecting multiple biomarkers from a single drop of blood. Although this founding claim has ultimately turned out to be just a pipe dream, investors are still injecting a great deal of resources into start-up companies geared toward both ultrafast diagnostics and on-site point-of-

care test (POCT) applications. With this trend, the model of patient-centered diagnostics continues to gain traction, moving away from the centralized laboratory-based diagnostics.

The nucleic acid amplification test (NAAT) has been widely used in molecular research, genetic testing, forensics, agriculture and clinical medicine (Ballard and Ozcan, 2018; Park et al., 2014). NAAT is highly sensitive and specific even with a small sample size, since it can greatly amplify a few copies of a given nucleic acid (NA) segment (e.g., deoxyribonucleic acid [DNA] and ribonucleic acid [RNA]) paired to a specific target NA. Consequently, NAATs have become the gold standard in a broad range of applications ranging from forensics, food safety and agriculture to clinical diagnostics (Marx, 2015). One of the target NA amplification methods is polymerase chain reaction (PCR), which is the core technology behind most NAATs (Gill and Ghaemi, 2008), and has been widely used in diagnosing infectious diseases and in genetic

\* Corresponding author.

E-mail address: [bjun@konkuk.ac.kr](mailto:bjun@konkuk.ac.kr) (B.-H. Jun).

<https://doi.org/10.1016/j.bios.2019.111448>

Received 2 April 2019; Received in revised form 31 May 2019; Accepted 17 June 2019

Available online 18 June 2019

0956-5663/ © 2019 Elsevier B.V. All rights reserved.

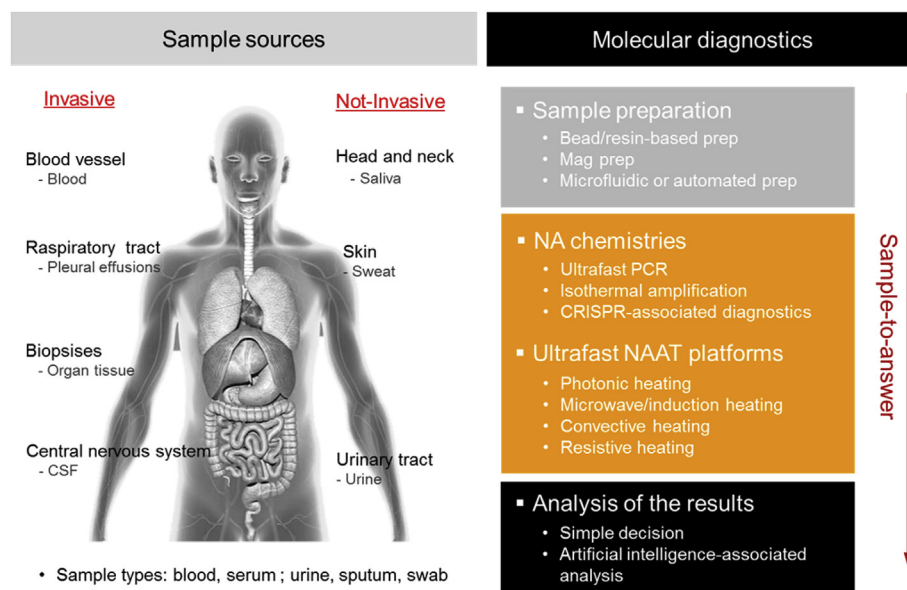


**Fig. 1.** The consecutive steps in the current trend of molecular diagnostics. The nucleic acid (NA) can be extracted from diverse types of the sample such as whole blood, tissue or urine. Then NA amplification process is performed relying on repeated thermocycling or isothermal amplification with the target NA. Finally, the quantification procedure performed with integrated optical detection system with high precision and resolution. In the near future, the analysis and decision process can be extended to AI-based diagnosis with more accurate standards or references.

testing of a large variety of sample types (Saiki et al. 1985, 1988a). PCR is based on the amplification, detection and quantification of a target NA sequence. However, the process of NA amplification in PCR requires certain thermal conditions for thermocycling that needs reliable and precise control. As a result, PCR typically runs under bulky and expensive equipment, requiring relatively large power consumption and lengthy turn-around times (TAT) of up to an hour or more. Alternative methods of NA amplification, such as isothermal NAAT (iNAAT), have therefore been developed recently. The iNAATs utilize specialized enzymes to perform a strand displacement that would otherwise require repeated thermal cycling (Craw and Balachandran, 2012). As such, iNAATs widen the option of developing POCT diagnostic platforms free from the complex thermal cycling steps and associated control.

This review first discusses the various methods of sample preparation and current NA amplification techniques, as well as relevant thermal cycling processes. Specifically, the main focus of discussion is on ultrafast NA amplification using various methods, including light-, radio frequency-, convective flow- and resistive-assisted thermal cycling, contrasting with the traditional Peltier-based methods. The basic mechanisms of each amplification approach are described to guide readers to more detailed information on the NA detection capabilities of the various platforms. Lastly, the design and engineering considerations of various innovative NAAT devices are explored, with attention being given to integrated sample preparation, artificial intelligence (AI)-assisted clinical decision-making and mobile healthcare networks, enabling next-generation ultrafast NA diagnostics.

## 2. Principles of sample preparation for NA diagnostics

### 2.1. Biomarkers in bodily fluids

Early diagnosis of a disease is important as patients have a better prognosis and more treatment options (Rodríguez-Enríquez et al., 2011). To allow timely treatment, extensive research has been conducted to discover early-stage biomarkers associated with various diseases. NAs, which include DNA and RNA, are the most important biomolecules in living organisms as they carry genetic information (Lee et al., 2018). As such, nearly all diseases possess a series of biomarkers associated with NA molecules (Ding and Mu, 2016; Lee and Jun 2019), and hence they have been used as essential biomarkers for the detection of various diseases, such as cancer, cardiovascular and infectious diseases, including acquired immune deficiency syndrome (AIDS), tuberculosis and malaria (Cao et al., 2017). Biomarkers obtained from

biological samples such as tissue, blood, urine and saliva, are essential for determining the concentration and copy number variation of target NAs (Chiappin et al., 2007; Malamud and Rodriguez-Chavez, 2011; Siravegna et al., 2017). Although the presence of pathogen's NAs in a whole blood sample represents a potential presence of pathogens in the body, the concentration of circulating NAs in the sample is extremely low, making them undetectable without amplification (Cao et al., 2017).

One of the most convenient sources for circulating biomarkers is the plasma fraction of blood. A low concentration of cell-free DNA (cfDNA) is normally detectable in plasma from healthy subjects, containing hundreds of genome copies per milliliter sample. Moreover, various studies on plasma genome, proteome, transcriptome and metabolome have allowed rapid expansion of diagnostic targets for numerous diseases. Nevertheless, a bench-top centrifuge is still required to produce an input plasma sample, even if a required volume is only a few microliters, which calls for a continued improvement of microscale separation methods of samples such as blood, plasma and tissues to develop integrated diagnostic devices for NA detection (Mielczarek et al., 2016). In the sample collection and preparation process, a readily applicable blood-dilution method is also needed, where *in vitro* hemolysis is a well-known source of abnormal variability in molecular diagnostics.

### 2.2. NA sample preparation

As shown in Fig. 1, many areas of the body are subject to disruption from bacterial or viral pathogens, which leads to the presence of biological components in the various bodily fluids and enables downstream NA-based detection. In most such instances, the sample preparation process can proceed in two steps, which are (i) cell, tissue and bacteria lysis; and (ii) NA extraction or purification. The conventional sample preparation includes sample filtration, centrifugation and dilution, which is typically achieved in an ordinary laboratory setting in time-consuming and labor-intensive multi-step processes. The cell lysis methods that are currently being used in microsystems can be broadly categorized into chemical, physical and electrochemical lysis. Chemical disruption uses a chemical reagent to break down the cell membrane and is a commonly used cell lysis method as it does not require any specific equipment. This chemical lysis typically utilizes detergents or alkali chemicals to disintegrate certain lipids and proteins inside the outer membrane of target cells. Next is physical lysis which can be thermal or mechanical. Thermal lysis is the most widely used NA extraction technique utilizing high temperatures to disrupt the cell

membrane. Heat generated externally by a heater or a PCR thermocycler is directly applied to target cells, resulting in the irreversible formation of pores within the cellular membrane. On the other hand, mechanical lysis can be performed in many different forms which employs cellular contact forces (e.g., pressure forces by using glass beads) to crush or burst the cell membrane to release its cytoplasmic contents (Cheng et al., 2017; Islam et al., 2017). Since biological cells are not rigid particles, sharp micro/nanostructures can be integrated within a microfluidic system to damage the cell membrane. Lastly, pores can be induced in a cell membrane via electrical/electrochemical lysis, which has been gaining popularity, as it is rapid and requires no agent (Lee et al., 2010; Pavlov et al., 2004). For example, hydroxide ions generated electrochemically by an electrode within a device can irreversibly porate the cell membrane and subsequently bring the intracellular contents to spill out. Since there are no chemical reagents involved, electrochemical lysis do not interfere with downstream assays. Nevertheless, the electric fields can be highly concentrated in a confined, small-scale geometry as in microfluidic chips.

Column-based extractions are widely used for cost-effective NA extraction methods due to their relatively rapid processing time (~30 min). To further reduce the process time, macroscale solid-phase extraction (SPE) methods have been developed which utilize magnetic/silica beads or ion exchange resins (Pham et al., 2017). However, the process of centrifugation or manual pipetting required by the methods render a device difficult to be automated. To facilitate automation, numerous research have focused on developing practical lysis and NA extraction protocols from samples that can be easily integrated to POCT (Mulberry et al., 2018). Although a variety of methods currently exist for chip- or micro-scale extraction from biological samples, to implement them in POCT designs is still a challenge due to a wide variety of specimen sources and of detectable ranges in target biomolecules. As shown in Fig. 2, the Prakash group at Stanford University described an electricity-free, ultra-low-cost paper centrifuge, ‘paperfuge’, which can be used in resource-poor settings. The paperfuge can attain a speed of up to 125,000 rpm (centrifugal forces of ~30,000g) and achieve the separation of pure plasma from whole blood in less than 1.5 min (Bhamla et al., 2017).

### 3. NAATs

#### 3.1. Polymerase chain reaction (PCR)

PCR amplifies copies of NAs for target biomarker identification and is a powerful tool for detecting NAs from viruses, bacteria or parasites in patient specimens, food and environmental samples even at low concentrations (Pavlov et al., 2004; Saiki et al. 1985, 1988a). Producing a new DNA strand *in vitro* requires three steps in PCR: (a) denaturation - to produce single-stranded DNA (ssDNA) as a template; (b) annealing - to bind the primer and thus initiate the synthesis of complementary DNA (cDNA) strands; and (c) extension - to synthesize new DNA strands by polymerase, yielding the double-stranded (dsDNA) product. After one cycle, two DNA strands are produced from single template, and the number of DNA molecules yielded by subsequent cycles doubles each time, as in a geometric series ( $2^n$  after  $n$  cycles), exponentially increasing the concentration of target DNA (Maurer, 2011). When the threshold cycle is reached after an  $X$  number of cycles, a cycle threshold ( $C_t$ ) value can be measured to estimate copy and cell numbers, which is a relative value of the concentration of target molecules in quantitative PCR (qPCR). Since there is an inverse relation between the number of cycles and the copy (or cell) number at which the amplicon is initially detected, the  $C_t$  value allows the estimation of cell or viral pathogen concentrations in clinical samples. A real-time PCR procedure can thus be standardized against a set of known target DNAs or cell concentrations, the values of which can be converted to quantify the results.

DNA polymerase, primers and probes are the three important elements for effective PCR-based diagnostics. Firstly, the thermal

denaturation of polymerase is an inherent limiting factor in PCR. The DNA polymerase of thermophilic bacteria such as *Thermophilus aquaticus* (*Taq*) is employed, since it is resistant to high temperatures (95°C) for the denaturation step and enzymatically active below 72°C for the annealing and extension steps, enabling the repeated thermocycling necessary for DNA replications. Secondly, the primer determines where DNA synthesis can be initiated. The size of the target DNA amplicon is a function of the distance between the two DNA primers, and the appearance of the amplicon is dictated by the presence of DNA sequences complementary to both the forward and the reverse primers. Effective primer design is essential for successful, high-yield PCR amplification, which can be accomplished by optimizing various factors such as guanine-cytosine (GC) contents, secondary primer structure, repeated primer sequence, primer length and melting temperature ( $T_m$ , the temperature at which 50% amplification of the target DNA has been reached, which is dependent on DNA sequence and length) (Arvidsson et al., 2008). Probes are the last important component in PCR. Various types, such as TaqMan probe, molecular beacon, Scorpion probe, etc., can be integrated into PCR to ensure reliable detection of target DNA. These probes utilize fluorescence energy transfer (FRET), a transfer of energy from a donor molecule in an excited state to an acceptor (Didenko, 2001). In general, when the probes are not hybridized to their complementary target, fluorescent and quenching dyes remain proximal to one another. These probes can also possess fluorophores of various colors, allowing the detection of multiple target sequences in the same reaction vessel (Tyagi et al., 2000).

**SYBR Green** Most real-time qPCR assays incorporate sensitive intercalating fluorescent dyes (SYBR, EverGreen, etc.) that bind non-specifically to dsDNA as it is produced (Fig. 3a). SYBR shows a number of characteristics such as spectral properties close to fluorescein, high sensitivity of 1,000-fold higher than ethidium bromide (EtBr), and high specificity to dsDNA that are far superior to EtBr. These characteristics, coupled with its cost-effectiveness and convenience, have made fluorescent dyes the most popular method for real-time PCR monitoring. However, they can yield false-positive results associated with non-specific amplicons, and such results of unintended products can hinder the detection of a true target.

**TaqMan probe** The problem with the false-positive results from SYBR was later resolved with the inclusion of internal probes (i.e., TaqMan probe) or with the introduction of the melting curve analysis to identify products. In particular, TaqMan probe can significantly reduce false-positive results by driving the internal site to anneal to its true target amplicon (Arya et al., 2005). As shown in Fig. 3b, TaqMan probes, which can be cleaved by *Taq* polymerase, are short and non-extendable oligonucleotide probes that include a fluorescent reporter dye at the 5' end and a quencher at the 3' end (Holland et al., 1991). When the two ends of the probe are in close proximity, the reporter and quencher dyes do not undergo FRET, and fluorescence emission does not occur. The oligonucleotide probe has a covalently bonded fluorescent reporter dye and quencher such as 6-carboxyfluorescein (FAM), tetrachloro-6-carboxy-fluorescein (TET), hexachloro-6-carboxy-fluorescein (HEX), or 2'-chloro-7'-phenyl-1,4-dichloro-6-carboxy-fluorescein (VIC), and a quencher dye including either 6-carboxy-tetramethylrhodamine (TAMRA) or 4-(dimethylamino)zoo benzene-4-carboxylic acid (DABCYL) at the 5' and 3' end, respectively (Didenko, 2001). As the *Taq* polymerase extends the primers, the exonuclease cleaves the hybridized probe and separates the reporter from the quencher during the PCR extension step. The increase in fluorescence signal is directly proportional to the amount of amplicon generated. These TaqMan probes are ideal for the detection of single nucleotide polymorphisms (SNPs) and for the quantitative analysis of methylated alleles (Liew et al., 2004; Zeschinck et al., 2004).

**Molecular beacons** Molecular beacons which possess a stem-and-loop structure (i.e., hairpin) are single-stranded oligonucleotide probes that emit a fluorescent signal when they bind to a perfectly complementary target sequence (Fig. 3c) (Tyagi and Kramer, 1996). The



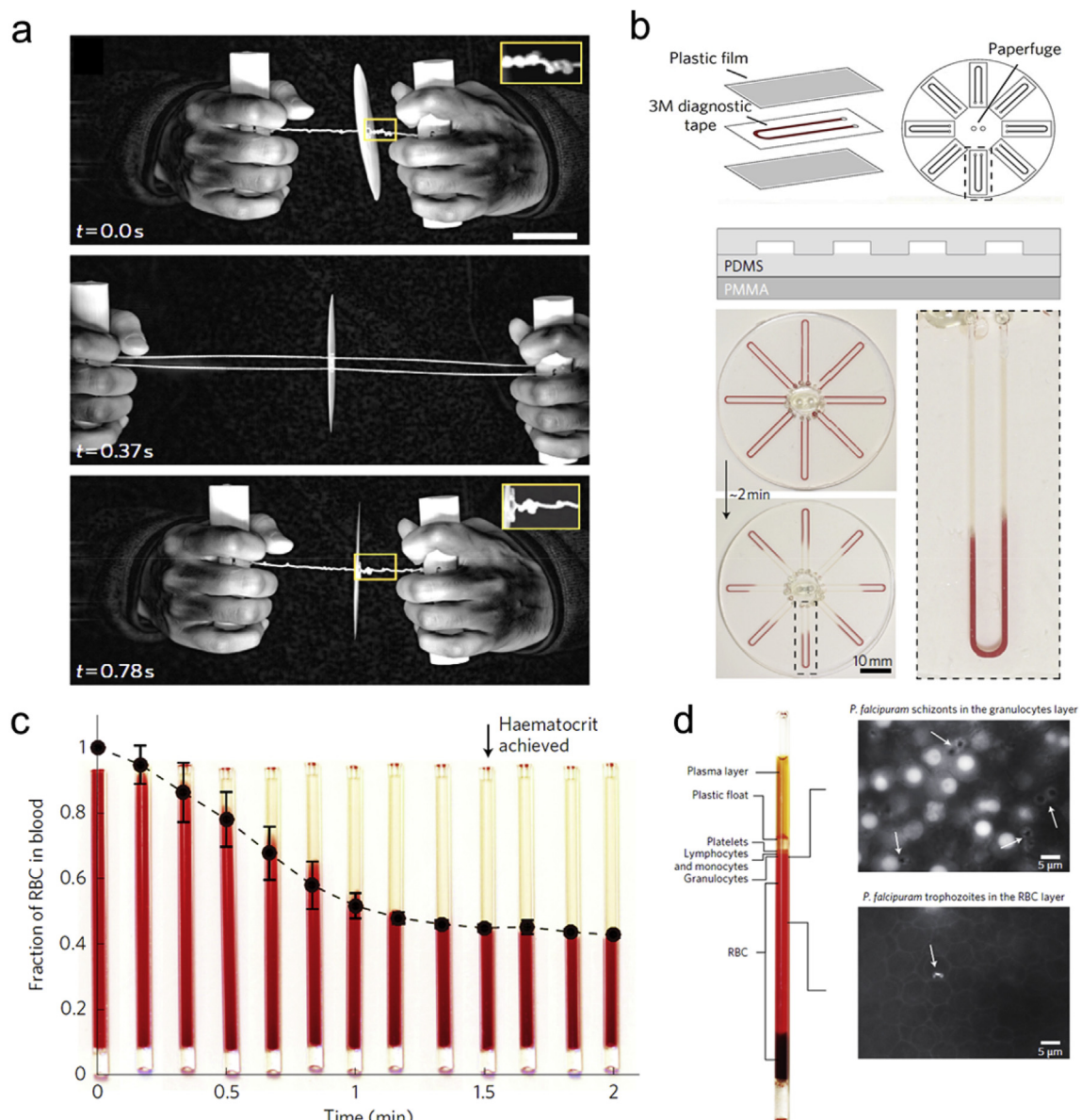


**Fig. 2.** Spinning dynamics-based paper centrifuge. (a) Images of a rotating paperfuge captured with a high-speed camera showing a succession of wound (top), and re-wound (bottom) states, for half a cycle. Materials used to construct the paperfuge include two paper discs, wooden handles, string, capillaries, capillary holders and plastic shims. (b) Kinetics of red blood cell (RBC) and plasma separation. (c) Separation of 8  $\mu\text{l}$  of blood plasma (per capillary tube) from whole blood occurred in less than 1.5 min. (d) Paperfuge application in malaria diagnosis. The parasite in *Plasmodium falciparum*-infected blood is rapidly visualized using a fluorescent microscope in specific density layers. Reprinted with permission from (Bhamla et al., 2017). Copyright 2017, Nature Publishing Group. (For interpretation of the references to color in this figure legend, the reader is referred to the Web version of this article.)

close proximity of a fluorophore and a quencher in the stem-and-loop configuration suppresses the reporter fluorescence based on the FRET mechanism. The loop portion of the beacon is complementary to the target sequence, while the stem portion is formed by the annealing of the two complementary sequences, forming the arm ends of the probe. In the absence of the target sequence, the stem-and-loop structure keeps the fluorophore trapped, and its excitation energy is transferred to the quencher and released as heat. Conversely, when the probe sequence of the loop hybridizes to a complementary target sequence during the annealing step, the probe-target complex forces the stem portion to unwind, resulting in a linear structure, separating the fluorophore from the quencher, and emitting fluorescence with increased intensity. Hybridization takes place in the annealing step of each PCR cycle, and the resulting fluorescence intensity is proportional to the amount of amplicon (Szuhai et al., 2001). The specificity of molecular beacons gained from their hairpin structure has been proved to be superior to the

TaqMan probe which relies on the exonuclease activity of DNA polymerase (Vet et al., 1999). This high specificity of the beacon is especially suited for the detection of point mutations in the presence of abundant wild-type DNA or even in living cells (Mhlanga and Tyagi, 2006; Mhlanga et al., 2005; Tyagi et al., 1998).

**Scorpion probe** Similar to molecular beacon probes, Scorpion probe is a single-stranded, bi-labeled fluorescent probe presenting a stem-and-loop configuration (Solinas et al., 2001; Whitcombe et al., 1999). As shown in Fig. 3d, Scorpion probes consist of a reporter dye (R) attached to the 5' end, a complementary stem-and-loop structure wherein the loop contains a probe sequence specific to the target, a quencher dye (Q), a blocker for DNA polymerase (B), and a PCR primer at the 3' end. At the beginning of qPCR, the polymerase extends the PCR primer and synthesizes the complementary strand of the specific target sequence, while the blocker prevents the polymerase from extending the PCR primer. During the next cycle, the stem-and-loop unfolds, and the loop

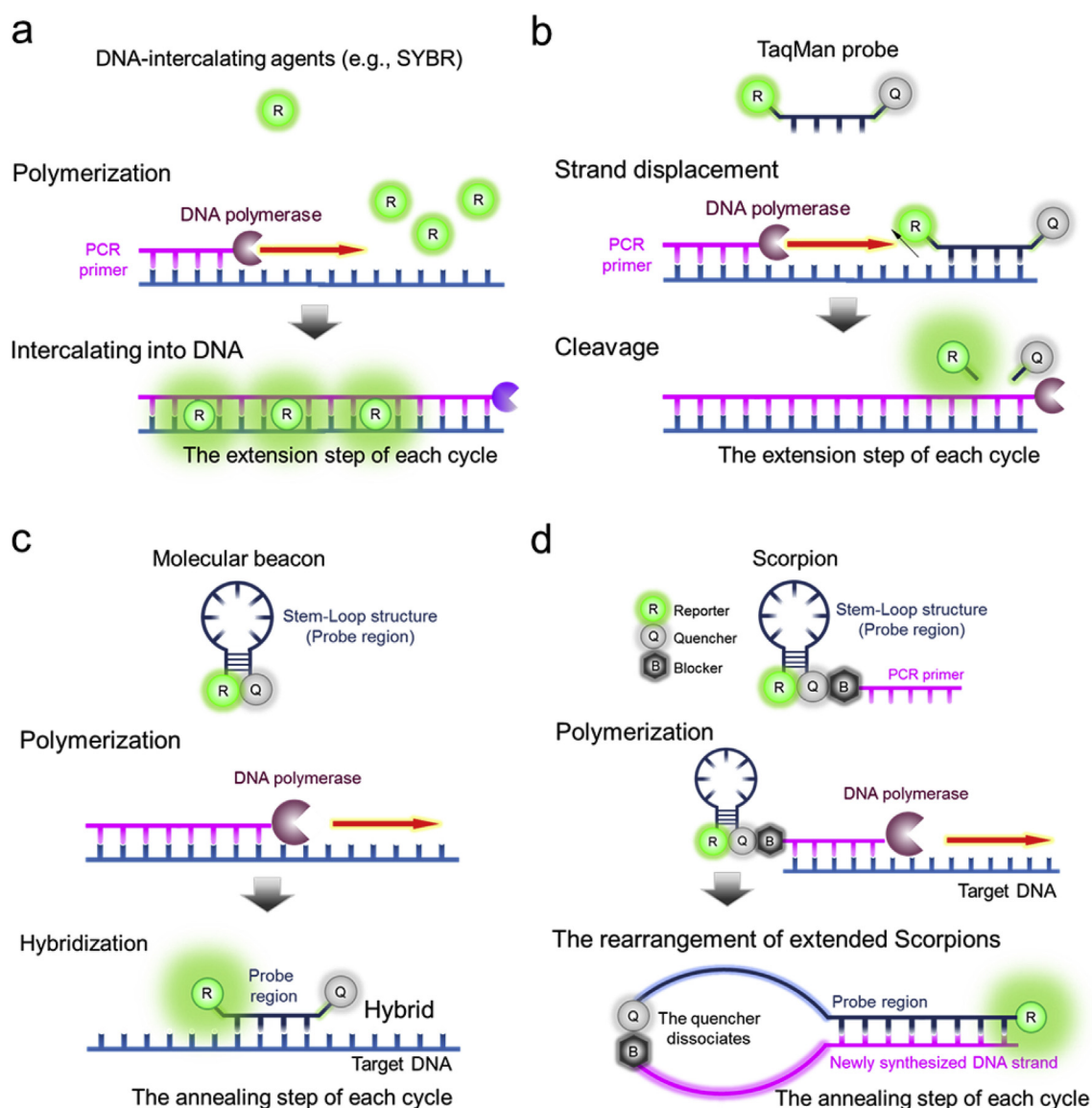


**Fig. 3.** The working principles of various molecular probes. (a) DNA-intercalating agents. During primer extension and polymerization, SYBR becomes intercalated within the double-stranded DNA, resulting in an increase in the detectable fluorescence level. (b) TaqMan probe hydrolysis during the amplification process. During PCR amplification, the probe anneals to the target DNA sequence, and Taq polymerase cleaves the probe, enabling an increase in fluorescence emission. (c) Molecular beacons. During the annealing step, beacons hybridize to the target DNA sequence, which changes beacon conformation and separates reporter and quencher dyes, resulting in fluorescence emission. (d) Scorpion probes. The probe sequence in the Scorpion loop structure hybridizes to the newly synthesized complementary target DNA from the PCR product. As the tail of the Scorpion and the PCR product are now part of the same DNA strand, the reaction is effectively instantaneous and yields a much stronger fluorescence signal.

region of the Scorpion probe hybridizes to the newly synthesized target sequence. With the hybridization, the reporter is no longer in close proximity to the quencher, and fluorescence emission can therefore take place and be detected through qPCR optics. Since the probe and primer are incorporated into a single-strand structure, the reaction kinetics of the Scorpion probe are extremely fast (Whitcombe et al., 1999). The reaction leading to fluorescent signal generation is instantaneous, which means that it occurs prior to any competing side reactions. This rapid kinetics enables a more reliable probe design, stronger signals, shorter reaction times and better discrimination than other conventional bi-molecular mechanisms.

### 3.2. Isothermal nucleic acid amplification tests (iNAATs)

Although PCR has become widely used in NA detection, it still requires thermocycling at 95°C to denature dsDNA, which has limited its

application in POCT. To circumvent the limitations of traditional PCR, great efforts have been made on developing isothermal NAAT (iNAAT) methods which are ideal candidates for POCT applications. iNAAT techniques use specific enzymes to perform dsDNA denaturation without the need for repeated thermal cycling. Among the available iNAATs, such as rolling circle amplification (RCA), strand displacement amplification (SDA) and nucleic acid sequence-based amplification (NASBA) still require an initial heating step (~95°C) to denature dsDNA, while a number of other isothermal techniques, such as recombinase polymerase amplification (RPA) or loop-mediated amplification (LAMP), can act directly on dsDNA without the heating step. Importantly, these non-PCR based methods operate at lower temperatures than conventional PCR, and do not require thermocycling, precise temperature control, nor high power consumption (Tsaloglou et al.). In the following section, the best-known iNAATs are briefly summarized in terms of their working principles and potential applications as a next-

generation molecular diagnosis method.

**Loop-mediated isothermal amplification (LAMP)** LAMP is one example of the iNAAT, which amplifies DNA with high specificity under isothermal conditions (60 to 65°C) (Tomita et al., 2008). LAMP employs only a single type of enzyme (*Bst* polymerase large fragment) and a set of specially designed primers which are 20–45 bp long and operate at the inner and outer sites of the template, as well as in the loop regions (Notomi et al., 2000; Tsaloglou et al.). Following advantages are shown in LAMP: (i) high specificity, originating from the use of six distinct primers, namely outer primers (forward and backward primers, FP and BP), inner primers (forward and backward inner primers, FIP and BIP), and loop primers (loop forward and backward primers, LF and LB), which utilize six separate binding regions on the target DNA; (ii) comparable sensitivity to that of nested PCR; and (iii) tolerance against inhibitory compounds (Kaneko et al., 2007; Notomi et al., 2015). It is the inner primers that initiate LAMP and possess a complementary sequence of the 5'- and 3'-terminals of the target DNA. The elongation steps are sequentially repeated by DNA polymerase-mediated strand displacement synthesis, using the single-stranded stem-loop regions at each end which serve as templates for the next round of DNA synthesis. This cycling process results in an accumulation of  $10^9$  copies of the final amplicon with multiple loops in less than an hour. Due to its large output, the fluorescence (i.e., SYBR) or turbidity method can also be used in LAMP amplicon detection. The turbidity method is a simple detection technique that utilizes the turbidity of magnesium pyrophosphate which is a by-product of DNA synthesis.

**Recombinase polymerase amplification (RPA)** RPA is a low-temperature isothermal method of amplifying specific target DNA using 3 types of enzymes including recombinase, DNA-binding protein and polymerase. At 37°C, recombinase and primer complexes promote strand displacement and primer binding at the target dsDNA sequence. The displaced strand is stabilized by ssDNA binding proteins. The primer is then extended by the polymerase. The two dsDNA products can be copied, resulting in exponential amplification. RPA has been applied to a variety of DNA targets (down to 10 copies), and the amplified targets have been detected in real-time analysis using intercalating dyes and specific fluorophore/quencher probes, as well as lateral flow assays (LFAs) (Asiello and Baumann, 2011). A digital microfluidic-based RPA platform has been demonstrated to quantify the presence of human immunodeficiency virus (HIV) in whole blood (Yeh et al., 2017). Recently, RPA was adapted to perform highly sensitive NA detection by capitalizing CRISPR enzymes with distinctive properties (Chertow, 2018). The Doudna group at UC Berkeley discovered that the CRISPR-Cas12a protein processes ssDNA threading activity in addition to processing dsDNA (Chen et al., 2018). The DNA endonuclease-targeted CRISPR trans reporter (DETECTR) method combined with RPA demonstrated high sensitivity recognition of human papillomavirus (HPV) in patient samples. The Zhang group at MIT developed a platform, specific high-sensitivity enzymatic reporter unlocking (SHERLOCK), which combines RPA pre-amplification with Cas13 to detect single DNA and RNA molecules (Myhrvold et al., 2018). Gootenberg et al. further improved NA detection by combining RPA and CRISPR into a multiplexed quantitative and highly sensitive detection system, which incorporates LFA for a visual readout (Gootenberg et al., 2018).

**Nucleic acid sequence-based amplification (NASBA)** NASBA is derived from transcription-based amplification which is very similar to self-sustained sequence replication (SSR) and transcription-mediated amplification (TMA) (Compton, 1991), and can be used to amplify RNA, including mRNA, tRNA and tmRNA, as well as DNA (Kumar et al., 2018). NASBA is carried out at a constant temperature of 41°C within a time period of up to 90 min by three types of enzymes, including RNase H, avian myeloblastosis virus (AMV) reverse transcriptase and T7 RNA polymerase. A major advantage of NASBA can be found in the synthesis of ssRNA, which can easily be hybridized to fluorescent-labeled probes without requiring any denaturation step. One disadvantage of NASBA, however, is the requirement of an initial heating step (95°C for DNA

and 65°C for RNA) to obtain accessible single strands for the main amplification step occurring at 41°C. During the initial phase, reverse DNA primers containing a T7 promoter region bind to any available target DNA sequence, and are subsequently extended by reverse transcriptase. The RNA from the resulting RNA-cDNA product is degraded by RNase H, leading to single cDNA strands. The remaining forward DNA primer hybridizes to the target DNA to synthesize a new template, which can be elongated by reverse transcription. During this cyclic process, each synthesized RNA strand will initiate a new round of duplication, leading to exponential amplification (Troger et al., 2015), which adds great versatility to NASBA. For instance, Gulliksen et al. described NASBA with a beacon probe in a microfluidic chip (Gulliksen et al., 2005), and Dimov et al. presented the on-chip purification and quantitative amplification of cDNA from an *E. coli* sample using NASBA (Dimov et al., 2008). The Dimov group was able to detect a target RNA sequence that contained organism-specific sequences, showed higher stability compared to mRNA, and had a high copy number in the bacterial cell. Nowadays, commercially available diagnostic products based on real-time NASBA can be found (Troger et al., 2015). BioMerieux (Marcy-l'Etoile, France) developed an automated NucliSENS EasyQ platform, which combines NASBA and real-time molecular beacon detection (Yager et al., 2006). Up to 48 samples can be run in parallel, offering target detection in less than 2 h.

**Rolling circle amplification (RCA)** The RCA is a highly specific isothermal amplification method which can replicate multiple copies of the circle DNA sequences by DNA and RNA polymerase to generate long ssDNA or RNA. It utilizes the bacteriophage  $\phi$ 29 DNA polymerase enzyme acting on circular DNA targets at a single temperature (37°C), a single DNA primer, and padlock probes (Gu et al., 2018). In RCA, the DNA primer hybridized to the circular ssDNA target sequence, then circular padlock probes used as a template can be replicated by  $\phi$ 29 DNA polymerase to produce a long ssDNA with numerous repeated units, which are equal to the circular DNA template. Because of its simplicity, accuracy, and efficiency, RCA was utilized for a promising tool as a signal amplification strategy. It permits sensitive and highly multiplexed assays for in-situ or microarray hybridization analysis because RCA-mediated amplified signals still localized at the microarray spots (Lizardi et al., 1998). For example, Schweitzer et al. describe the RCA-based microarray platform for multiplexed protein profiling (Schweitzer et al., 2002). As another approach, RCA and exonuclease III (Exo III) were utilized for the prostate-specific antigen (PSA) or carcinoembryonic antigen (CEA) detection (Qiu et al., 2018b; Zhang et al., 2018b). RCA reaction was achieved with  $\phi$ 29 DNA polymerase and T4 DNA ligase to amplify the long ssDNA which can construct the ssDNA/G-quadruplex/hemin structure. Then, G-quadruplex/hemin is released by the digestion of Exo III to generate the detectable signal which can be detected in the photoelectrochemical (PEC) sensing platform as low as 16.3 pg/ml of PSA. Similarly, Qiu et al. describe the RCA and strand hybridization-based fluorescence signal enhancement method for quantitative screening of lysozyme (Qiu et al., 2017b). The assembly of quantum dot and hemin/G-quadruplex via RCA to produce numerous repeated oligonucleotide sequences was used for signal amplification. Also, the bio-bar-code-based PEC immunoassay through RCA was also presented by Zhang and colleagues (Zhang et al., 2018a).

**Strand-displacement amplification (SDA)** The SDA is an isothermal *in vitro* NA amplification technology based on a restriction endonuclease (HincII), exonuclease deficient DNA polymerase (exo<sup>-</sup>klenow), and four sequence-specific primers (Dean et al., 2002; Walker et al., 1992). In particular, this SDA method relies on functional primers incorporating both endonucleases target regions and target recognition (Craw and Balachandran, 2012). In details, SDA reaction carried out by two functional enzymes which are a restriction endonuclease to nick the unmodified sequence of target DNA, forming the recognition site and DNA polymerase I which elongates four primers (Kumar et al., 2018). Particularly, the nicking of the unmodified strand allows the polymerase for the existing strand displacement and incorporate a new



amplicon. Thus, this strategy is suitable for exponential amplification. For instance, SDA was used for clinical diagnosis for CT/NG (*C. trachomatis* and *N. gonorrhea*) by a semiautomated real-time detection system (Little et al., 1999). Also, the isothermal SDA was utilized for the sensitive detection of the antibiotic residue by coupling the polyaniline nanowires-functionalized reduced graphene oxide (Zeng et al., 2018a). Similarly, Zheng et al. reported new assay platform which is the palindromic molecular beacon (PMB) coupled with SDA for the signal amplification and the photoelectrochemical (PEC) sensing platform for the detectable signal generation (Zeng et al., 2019a). This biosensor platform can efficiently promote the target recycling and the signal amplification to detect low-concentration of biomolecules (e.g., Kanamycin).

**Hybridization chain reaction (HCR)** The HCR is a simple and efficient isothermal non-enzymatic amplification strategy, which offers a probe-amplification for the rapid detection of target DNA (Dirks and Pierce, 2004; Evanko, 2004). Recently, diverse schemes and protocols based on HCR approaches have been constructed to apply for the diverse NA-related *in situ* or *in vitro* sensing platform. In an HCR, target DNA triggers a self-assembly cascade of hybridization events between two hairpin probes, leading to the formation of a nicked ssDNA with numerous repeated units until the hairpins are exhausted. In addition, HCR can effectively reduce false-positive results and cross-contamination due to probes-based amplification (Bi et al., 2017). Thus, HCR exhibited great potential as a signal amplification strategy without thermal cycling which offers excellent flexibility, simple operation, and easy construction.

For, Li et al. reported the application of the HCR in localizable imaging of microRNAs in living cells via HCR based enzyme-free signal amplification approach (Li et al., 2016a). Zeng and colleagues described the photoelectrochemical (PEC) biosensor based on branched HCR (bHCR)-mediated signal amplification to detect low abundance antibiotics (Zeng et al., 2019b). The bHCR strategy enabled to produce hyper-branched self-assembly of the nanoparticle-DNA hybrid network through the hybridization event with two hairpin probes, resulting in the exponential signal amplification. As another example, the HCR was employed to significantly enhance signal intensity combining nano-transducer such as upconversion nanoparticle (UCNP) and gold nanoparticle (GNP) (Gao et al., 2017; Qiu et al., 2018a). The HCR/SDA-based electrochemical aptasensor was also demonstrated to detect the kanamycin with high sensitivity down to 36 fM (Zeng et al., 2018b). In the presence of target molecule, hybridization events via HCR, SDA, and nicking endonuclease (Exo III) can be triggered to generate an electrochemical signal. Similarly, Zhou et al. constructed highly sensitive PEC aptasensor based on the target-triggered HCR (Zhou et al., 2018). Also, HCR was applied for the immune-HCR based sensitive biosensing strategy to recognize target proteins such as IgG and PSA (Zhang et al. 2012, 2017).

As we mentioned above, many of the isothermal amplification techniques currently available, but other novel strategies are also reported. For example, a label-free colorimetric assay combined with a nicking enzyme-mediated signal amplification approach was described by Liu and colleagues (Liu et al., 2014). Hou et al. reported that  $\lambda$  exonuclease cleavage reaction can be used to trigger the catalytic assembly of molecular beacons, resulting in a significantly amplified fluorescence signal. Taking advantage of the efficient enzyme reactions, the detection limit toward T4 polynucleotide kinase (PNK) was determined as 1 mU/ml (Hou et al., 2014).

### 3.3. Shift of trend towards ultrafast NAAT

Conventionally, thermocycling is performed through programmed heating and cooling of metallic blocks in a PCR tube via conduction-based heat transfer onto thermocyclers based on Peltier elements (Erickson et al., 2003). This method requires either physical contact or close proximity between a heated surface and a fluid to allow heat

transfer to occur. One advantage of Peltier elements is that they are well understood, thoroughly tested and readily available at a low cost, in addition to their lifespan of thousands of cycles. However, several drawbacks can be found. First is that they show relatively slow ramp rates (1.5–3°C/sec) and lengthy TAT of typically an hour or more, due to multiple heat transfer cascades taking place through the intermediate materials. Another disadvantage of Peltier modules is their high power consumption (typically 200–1000 W), which makes them unsuitable to be implemented in a POCT format (Miralles et al., 2013).

Significant advancements have been made in terms of NAAT reagents and thermocycling instruments. The main trends in NA diagnostics are shifting towards ultrafast NAATs, sample-to-answer diagnostics (e.g., the cell to Ct value concept) and miniaturized POCT device configurations. In particular, ultrafast PCR analysis is beneficial in medical diagnosis and treatments, in food safety assessments and even in national security services, for instance, airport securities (Marx, 2015). For this purpose, thermocyclers have also evolved away from Peltier-based PCR instruments (Saiki et al. 1986, 1988b) to fast and hot air-based thermocyclers (Wittwer et al., 1989). Recent advances in the academic and industrial fields have shown various features of ultrafast PCR. For example, the analytical run time of PCR has been reduced to 10 min or under (down from 60–90 min) through new thermocyclers based on innovative heating-cooling mechanisms and newly developed high-speed polymerase (Maltezos et al., 2010; Ullerich et al., 2017). In terms of PCR reagents, the Wittwer group has demonstrated that it is possible to use modified PCR protocols to achieve ultrafast PCR results without sacrificing performance (Farrar and Wittwer, 2015). Key factors that enable ultrafast PCR can be summarized as rapid thermocycling, low material heat capacity, high thermal conductivity and high-speed polymerase (Herold et al., 2009).

Various new thermocyclers have been developed for NAATs, showing attractive features such as compact size, improved heating and cooling rates, and reduced amplification times (Farrar and Wittwer, 2015; Neuzil et al., 2006). As a concept for low-cost and portable qPCR, Mulberry et al. described a 3D-printed, real-time PCR instrument for infectious disease diagnostics (Mulberry et al., 2017). The 3D-printed qPCR device is automated by closed-loop feedback thermal controls and time-coordinated fluorescence readings. The device is portable (12x7x6 cm, 214 g), battery-operated and capable of successfully detecting various concentrations of lentivirus, a class of retrovirus that includes HIV, via reverse-transcription and PCR. Currently, several vendors, such as Roche, Bio-Rad Laboratories, ThermoFisher, Cepheid, Analytical Jena, etc., have also launched their own commercial ultrafast or sample-to-answer PCR instruments (Ding and Mu, 2016). For example, the LightCycler (Roche, Switzerland) employs glass capillaries instead of plastic tubes to achieve more efficient heat transfer (Starr et al., 2015). The SmartCycler (Cepheid, USA) allows an individual control of thermocycling characteristics of each reaction well. In addition, Cepheid developed the GeneXpert, a fully automated qPCR platform, which performs sample processing to selectively detect HIV RNA in whole blood (Oyebanji, 2013; Semper et al., 2016; Waltz, 2017). The company has also offered a self-contained PCR laboratory on a portable cartridge with multiple PCR chambers that can perform different functions.

## 4. Ultrafast thermocycling methods

Although not as widely applied as the conductive temperature control approaches via thermoelectric modules (e.g., Peltier elements) described above, various heating methods offer significant benefits - from high-speed and low power consumption to ease of integration in sample preparation applications. The following section presents several heating approaches, including light-assisted heating (e.g., infrared, laser, LED and solar thermal), microwave heating via electromagnetic radiation, induction heating, convective flow heating and resistive heating.

#### 4.1. Light-assisted thermocycling

The most common approaches to temperature control rely on heat conduction as the means of heat transfer. Recent innovative designs have employed a light-assisted heating method as shown in Fig. 5a–c. These configurations require light sources, lenses and filters, as well as positioning of the PCR reaction fluid at an appropriate focal distance in the optical system. Infrared (IR) non-contact heaters are the most widely explored heating method in the literature (Easley et al., 2006). IR heaters are very efficient, delivering an impressive heating ramp rate. When using an IR laser or laser diode, the beam from the IR source is focused onto the reaction fluid. The IR energy is selectively absorbed by the aqueous reaction fluid, but the tube housing the energy is not heated to the same extent, as water absorbs IR light more efficiently than the other elements (Yu et al., 2012). The heating energy is provided directly to the reaction fluid and none is wasted by a heat spreader, thermal transfer medium, or surrounding plastic tube or chip. A disadvantage of this method is additional optical components, which tend to be bulky and is required to focus the IR energy on the reaction fluid. Focusing the IR beam reliably on the reaction volume requires a tight range of tolerance in the mechanical design, which entails additional complexity. For instance, Oda et al. reported the use of a tungsten lamp as an IR radiation source with temperature ramping in a micro-chamber (between 94 and 55°C), executed as rapidly as 10°C/sec for heating and 20°C/sec for cooling, respectively (Oda et al., 1998). A single cycle could be achieved in as fast as 17 s, wherein the configuration involves lenses, filters and solenoid-gated compressed air cooling. For the reaction to effectively occur, the setting also requires positioning of the PCR reaction fluid at an optimal focal distance. In another example, Burger et al. described an IR thermocycler to perform PCR with a centrifugal microfluidic disk made from cyclic olefin copolymer (COC) (Burger et al., 2011). The system involves an IR ring heater with a closed-loop temperature control via a wireless temperature sensor. PCR is carried out by direct heating of the PCR reagent with IR and forced-air ventilation, coupled with a disk rotation frequency from 3 to 30 Hz.

The Erickson group at Cornell University demonstrated a portable sunlight-assisted NA quantification platform which can be used on-site or in resource-limited environments (Snodgrass et al., 2018). As shown in Fig. 5d, this TINY (Tiny Isothermal Nucleic acid quantification sYstem) platform leveraged a phase-change material (PCM) to absorb and release latent heat generated from sunlight. The PCM (PureTemp 68, Entropy Solutions, USA) is inserted between two insulating cylinders to ensure a constant temperature for LAMP following the melting stage at 68°C. This portable TINY iNAAT device was used to diagnose Kaposi's sarcoma (KS), which is caused by the KS-associated herpesvirus (KSHV). The authors compared the performance of their TINY device with that of a commercial qPCR instrument. The agreement between TINY and qPCR results was 41/42 (98%) on a binary decision (detectable/not-detectable) in assays on 42 skin biopsies to find 8 patients negative (Fig. 4d, iii). Similarly, a portable, solar-powered microfluidic PCR platform was reported which employs solar-thermal energy to produce spatially modulated thermal patterns (Jiang et al., 2014). These solar PCR systems therefore can promote development of on-chip PCR and a light-weight and long-life device for POCT diagnostics.

In another approach, the photothermal effects of metal nanostructures, including gold nanoparticles (AuNPs) or thin Au film, can be utilized for ultrafast heating in NAATs. As shown in Fig. 5b and c, heating is localized at the nanoparticles, while the bulk of the solution is held at a constant temperature. This allows faster heating and cooling ramps compare to the conventional PCR, showing results much rapidly. For example, Lee et al. reported the use of gold bipyramid nanoparticle (AuBP)-based plasmonic thermal cycling for quantitative real-time PCR without the photobleaching of dye (Lee et al., 2017). This IR LED-driven photothermal heating approach was used for monodisperse PEG-Si-AuBPs, which have a higher absorbance coefficient than nanorods or

nanospheres (Navarro et al., 2014). When AuBPs (resonant wavelength of 846 nm) are exposed to IR LEDs, they act as a plasmonic heat converter to absorb photonic energy and convert it to heat, thereby increasing the temperature of the surrounding fluid (Webb and Bardhan, 2014). This plasmonic photothermal cycling exhibited rapid thermocycling of 141 s/30 cycles and heating and cooling rates of 16.6°C/sec and 9.4°C/sec, respectively. Despite the presence of gold, this approach was cost-effective (< \$0.01/reaction) and ready to be used with no further optimization of the existing PCR protocols. Similarly, Roche et al. developed an ultrafast (54-sec) plasmonic qPCR (Roche et al., 2017). The plasmonic qPCR employs very efficient heat transfer of optically irradiated metallic AuNPs, achieved by the photothermal heating of AuNPs in a thin-walled glass tube via a heating laser at 650 nm. As shown in Fig. 5e, a commercial, ultrafast laser PCR with a pulsed laser was developed by GNA Biosolutions (Germany) to selectively heat AuNPs functionalized with target-specific primers. The DNA targets were annealed to specific primers on the AuNPs, then DNA polymerase was bound for extension. Repeated laser pulses controlled the speed of PCR and amplified the target DNA (GNA Biosolutions GmbH), delivering real-time results in 10 min or less with as low as 2 copies/reaction. Researchers, notably the Lee group at the University of California Berkeley, have made great efforts to accelerate ramp rates through a blue LED-driven plasmonic heating method (Son et al., 2015). Thin Au film-based photonic thermal cycling was accomplished within 5 min, with ramp rates of 12.8°C/sec for heating and 6.7°C/sec for cooling, respectively. Similarly, Li et al. reported a photonic thermal cycler via magnetic nanoparticles (MNPs) (Li et al., 2016b). This photonic PCR system is composed of a NIR laser diode (808 nm, 460 mW) and Fe<sub>3</sub>O<sub>4</sub> MNPs that serve as a light-to-heat converter. A two-step PCR protocol for a 4977-bp fragment was completed within 420 s/30 thermal cycles in 10 µl of PCR mixture. This photonic PCR system demonstrated real-time qPCR detection through integration with a 450 nm blue LED for SYBR fluorescence (excitation: 488 nm; emission: 520 nm) and a highly sensitive complementary metal-oxide-semiconductor (CMOS) camera.

#### 4.2. Microwave/induction assisted thermocycling

Microwave-assisted dielectric heating is an attractive candidate for ultrafast heating method (Fig. 6a). Microwave heaters share some of the advantages of IR heating. In theory, the microwave heating system could be used to heat fluids directly with up to 95% efficiency owing to its preferential heating capacity (Garg et al., 2008; Orrling et al., 2004). For instance, aqueous solution or body fluids are mainly composed of suspended chemical and biochemical molecules, and is a good absorber of electromagnetic waves in the frequency range of 300 MHz to 300 GHz (wavelength 1 cm to 1 m) (Bradshaw et al., 1998). The advantage of the method is that the microwave energy can be delivered directly to the aqueous solution with little or no absorption from the substrate materials (e.g., glass or plastics). Specifically, due to the thermal inertialess nature of microwave heating, enhanced thermocycling rates (i.e., ultrafast rates of heating and cooling) and reduced reaction times can be achieved compared to the conventional techniques. The complex hardware system however is a major disadvantage. More efforts are still required to miniaturize, for instance, the microwave power source, microwave signal generator, etc. Shaw et al. developed a microwave-mediated non-contact thermocycler for DNA amplification that exhibits a heating ramp rate of 65°C/sec with an average power consumption of 500 mW (Shaw et al., 2010). Although a very small volume (0.7 µl) was used in the PCR, the values of high ramp rate and low power consumption are quite impressive. A microwave-assisted heating of a lab-on-a-chip device was described by Marchiarullo et al., who performed thermal cycling on 1 µl of PCR mixture to amplify a 520-bp fragment of λ-phage genomic DNA. The dielectric heating was achieved with a heating ramp rate of 40°C/sec and 7 W of DC power (Marchiarullo et al., 2013).



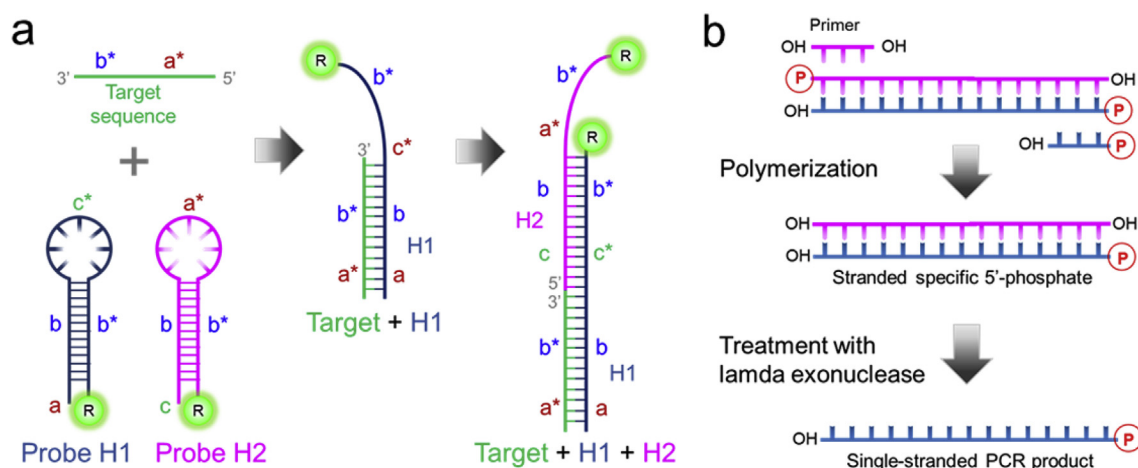


**Fig. 4.** The working principles of HCR and Lambda exonuclease-based detection. (a) Schematic illustration of the hybridization chain reaction (HCR). Addition of a target single-stranded DNA to two hairpin probes triggers to undergo a chain reaction events by alternating two hairpin probes polymerization. HCR amplification could be incorporated in various sensor platforms for a wide range of small molecules. (b) Lambda exonuclease-based NAAT. Lambda exonuclease is a highly active 5' exodeoxyribonuclease that can specifically digest the 5' phosphorylated strand of dsDNA. The resulting single-stranded product can be used for downstream assays such as sequencing or sensor platform.

Several authors have used induction heating as an alternative method for thermocycling (Debjani Pal and Venkataraman, 2002; Liu et al., 2011; Pal et al., 2004). As shown in Fig. 6b, the induction heating system is composed of a coil and an induction generator which generate a square wave pulse. Induction heating generally occurs through an electromagnetic field which generates heat and transfers it to a metal heat spreader, sample tubes or chips, from which heat can subsequently be transferred to a sample fluid. The overall heating and cooling rates, as well as the power consumption, rest somewhere between the rates of the Peltier and the thin-film resistive heating systems. For example, Kim et al. described a polydimethylsiloxane (PDMS)-based microheater with embedded magnetic nanoparticles (MNPs) as a heating element (Kim et al., 2010). The MNPs - superparamagnetic iron oxide ( $\text{Fe}_3\text{O}_4$ ) - were embedded in the PDMS at 10% and generated heat under an externally applied AC magnetic field. Similarly, Chen et al. demonstrated a wireless induction heater-based centrifugal microfluidic platform, as shown in Fig. 6b (Chen et al., 2013). One commercialized example of induction heating is the MIC thermocycler (BioMolecular Systems, Australia) which uses magnetic induction to heat samples and fan forced air to cool them (Fig. 6c). The MIC real-time thermocycler can deliver results through rapid heating and cooling, with up to 35 cycles under 25 min. In addition, the mechanism of rotary magnetic induction ensures centrifugation to spin down the sample in a tube, ensuring condensation by preventing evaporation (Roy et al., 2013).

#### 4.3. Convective flow-assisted thermocycling

Buoyancy-driven natural convection phenomena offer an attractive way to overcome the limitations of conventional thermocyclers (Agrawal and Ugaz, 2007; Shu et al.). Fig. 7a and b depict the basic mechanism of convective flow and the appropriately designed reaction geometry (e.g., a cylindrical cavity or closed loop) for convective heating through a static temperature gradient. A key element of this design is an architecture that allows the pseudo-isothermal operation of the entire thermocycling process by maintaining a heater at a constant temperature (Muddu et al., 2011). A simple design can be conceived where a PCR fluid is confined in a cylindrical volume, maintaining the temperature at the bottom higher than at the top. This would cause the fluid to flow in the entire reaction space and enable the PCR reagents to circulate through optimum temperature regimes. This arrangement would be highly advantageous in thermocycling, as it would eliminate the need for active heating and cooling, thus simplifying the instrument

design. However, to make it suitable for a real-time PCR requires reaction containers of various shapes, including tubes, cylinders or close-loop reactors, which would need to be stable at high temperatures as well as optically transparent. In addition, surface pretreatments would be required to minimize nonspecific binding.

Agrawal et al. demonstrated a triangular path-based convective PCR in which thermocycling is passively actuated by a unidirectional convective flow generated in response to an imposed thermal gradient (Agrawal et al., 2007). As shown in Fig. 7c, Qiu et al. reported a convective PCR in a capillary tube via a chemically-heated thermal process without electrical power (Qiu et al., 2017a). The amplification of H1N1 was achieved when the reagents in the capillary tube were spontaneously and repeatedly circulated through different temperature zones. Ugaz and Krishnan from Texas A&M University presented a convective flow PCR system arrayed in a multi-well cavity (5x5 wells) (Ugaz and Krishnan, 2004). This approach uses a Plexiglas PCR cartridge incorporating a 5x5 array of cavity chambers sandwiched between a metal bottom plate as a heating source and a top plate connected to flowing water for cooling. This cavity-based convective flow PCR system achieved PCR run times as short as 15 min using 30  $\mu\text{l}$  volumes to amplify a 474-bp region associated with the human  $\beta$ -actin gene. In a similar way, Shu et al. described that a handheld convective-flow PCR system for direct sample-to-answer NA analysis in real-time detection as shown in Fig. 7d (Shu et al., 2017). This system consists of a magnetic bead-based photothermal lysis for sample preparation, a closed-loop convective-flow PCR and a real-time fluorescence signal detection. The NA amplification was achieved in less than 25 min with a dynamic range from  $10^6$  to  $10^1$  copies/ $\mu\text{l}$ . The commercial LightCycler (Roche), based on thermocycling with rapid air convection, was developed by Idaho Technology (Heginbotham et al., 2003). The thermocycling of the LightCycler is achieved through forced air, using a hot hair dryer for heating and a household vacuum for cooling.

#### 4.4. Resistive heating-based thermocycling

Recently, numerous types of thin metal film-based or thermal block-based external resistive heaters have been used more widely for ultra-fast thermocycling in combination with a miniaturized microfluidic format. Generated heat energy is proportional to the electric current and the resistance of an ohmic conductor, and heating materials can easily be prepared on a solid or flexible substrate, using various physical or chemical deposition methods. Thus, this type of resistive

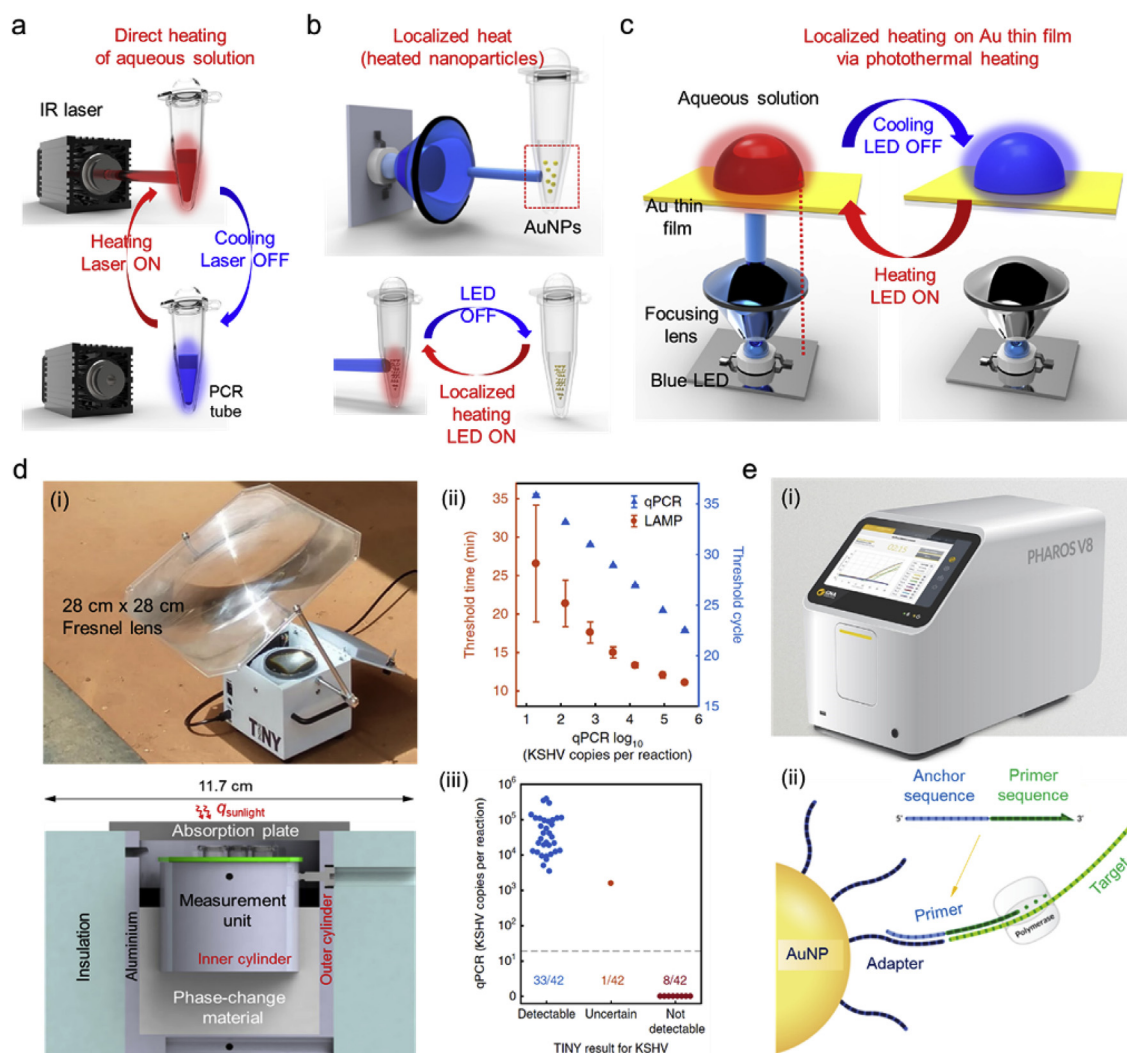


**Fig. 5.** Unconventional light-assisted heating system for thermal cycling. (a) Infrared (IR) heating-based thermal cycler. (b) LED-based plasmonic thermal cycler using a thin gold film as a light-to-heat converter and LEDs as excitation light. (c) Thin Au film-based plasmonic thermal cycler. Light is emitted from the light sources and then focused on the reaction volume by a lens. Photonic light energy is differentially absorbed by the aqueous solution, thin Au film or Au nanomaterials, respectively. The photonic energy is converted into heat for nucleic acid amplification applications such as PCR and isothermal amplification. (d) Concentrated sunlight-assisted portable PCR instrument. (i) TINY (Tiny Isothermal Nucleic acid quantification sYstem) heated via concentrated sunlight. TINY heated via phase-change material-based heater from sunlight (top). Cross-section of the temperature-controlling unit. After heat collection, the outer aluminum cylinder is covered with the insulation unit to minimize heat loss. (ii) and (iii) show the amplification performance of TINY. (ii) Standard curves for LAMP with TINY and with qPCR as a control instrument, respectively. (iii) TINY and qPCR agreement for clinical samples. Reprinted with permission from (Snodgrass et al., 2018). Copyright 2018, Nature Publishing Group. (e) Laser PCR instrument developed by GNA Biosolutions (Germany). In the laser PCR, AuNPs are functionalized with target-specific primer. Pulsed laser irradiation of colloidal AuNPs enables ultrafast local heating of the homogeneously dispersed AuNPs. (For interpretation of the references to color in this figure legend, the reader is referred to the Web version of this article.)

heating, which is also known as 'Joule heating', can be monolithically integrated into a variety of microfluidic lab-on-a-chip (LOC) formats. Resistive heating-based thermal cycling methods have the following advantages: (i) the ramping rates of heating and cooling are proportional to the applied electric current, which confers precise and direct control of temperatures; and (ii) the heating components and the multi-phase sample preparation modules can be integrated into the miniaturized single platform, minimizing the overall complexity and physical dimensions of the hardware. However, several engineering considerations need to be addressed in this approach, such as thermal constraints of the materials, unwanted water evaporation, non-specific reactions in the microfluidic PCR chamber due to the high surface-to-volume ratio, and physical contact with the heating element (Debjani Pal and Venkataraman, 2002). The bonding methods of the various materials (e.g., plastics, glass and silicon) should also be considered according to their ability to withstand high temperatures (e.g., denaturation

temperature of 95°C) (Asiello and Baeumner, 2011).

Fig. 8a shows the continuous-flow microfluidic PCR (CF PCR) configuration. The PCR fluid is forced to circulate through two or three temperature zones at a constant velocity in a microfluidic channel. The thermal cycling run time is proportional to the length of the micro-channel and to the speed of the fluid flow, but not to the thermal constant of the system (Kopp et al., 1998). Kim et al. reported a CF PCR with 3 separated temperature zones, corresponding to the 3 PCR thermocycling steps (Kim et al., 2006) where the thermocyclers consisted of a PID temperature controller, sensors and 3 heating modules. The CF PCR chip showed a short run time (~30 min in 30 cycles) and offered a small sample volume and a low cost. Similarly, a rotary zone thermal cycler was developed which could move the PCR reagent (Bartsch et al., 2015). Neuzil et al. described a thin-film heater-based ultrafast real-time PCR system consisting of a micro-machined silicon cantilever terminated with a disc (Neuzil et al., 2006). A PCR sample encapsulated

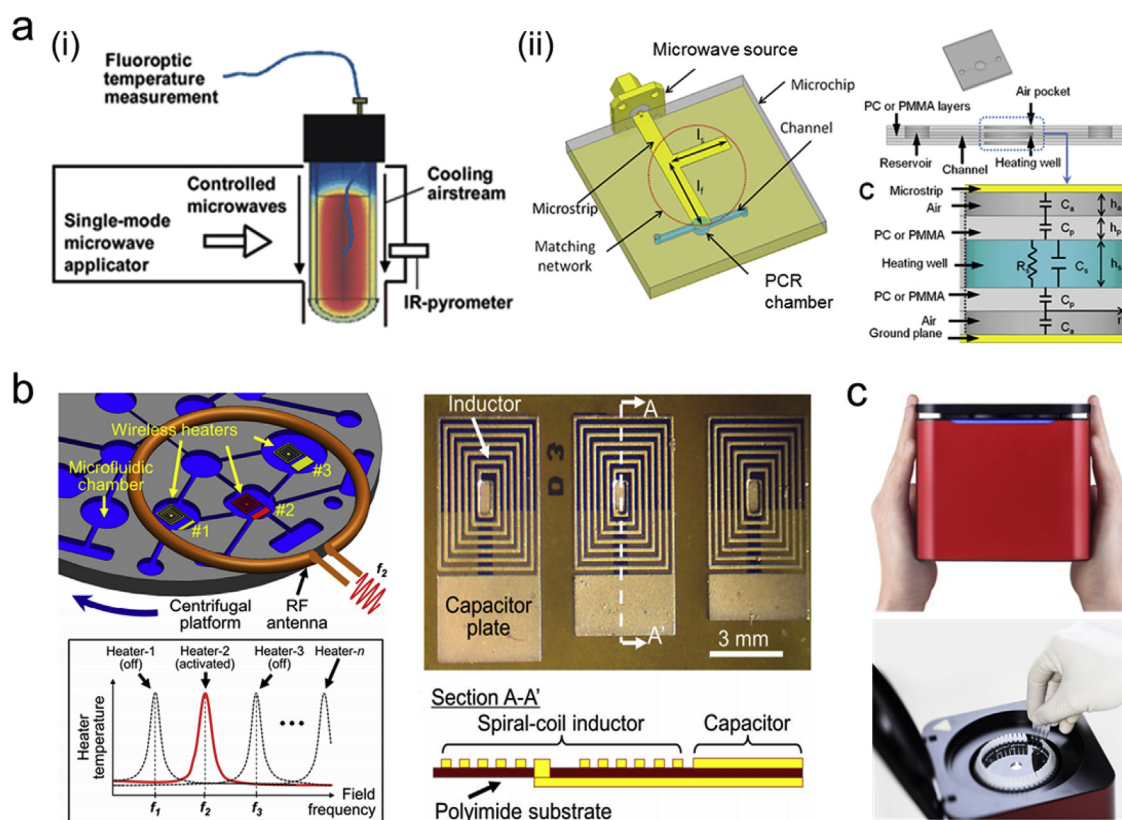


**Fig. 6.** Schematic illustration of microwave or induction-based thermal cyclers. (a) Experimental set up for microwave thermocycling. (i) Milliliter-scale PCR setup via microwave thermocycling. Pulsed microwave irradiation at 2450 MHz was applied for thermocycling. (ii) Microwave heater integrated microchip and microstrip matching network for efficient transfer of radiofrequency (RF) energy to PCR reaction chamber. Reprinted with permission from (Marchiarullo et al., 2013; Orrling et al., 2004). Copyright 2004 and 2013, Royal Chemical Society. (b) Wireless activation of micro resonant inductive heaters integrated into centrifugal microfluidic chip. Heater 2 is activated using an RF field by tuning its frequency to the resonant frequency of the heater. Reprinted with permission from (Chen et al., 2013). Copyright 2013, IEEE. (c) MIC PCR system (BioMolecularSystems, Australia) with magnetic induction-based thermocycler.

in mineral oil was dispensed onto a silicon disc, achieving 40 PCR cycles in less than 5 min 40 s, with a heating rate of 175°C/sec and a cooling rate of 125°C/sec.

The Mathies group advanced the portability and integration of a Joule-heated temporal thermocycling device as shown in Fig. 8b (Liu et al., 2011). This resistive heater-based PCR system was able to generate 9-plex target profiles by amplifying DNA detection through capillary electrophoresis (CE). Similarly, Kaigala et al. developed a fully integrated microfluidic design combining a thin Pt-film resistive heater, a pneumatic valve for fluid handling and CE in a 600 nl sample (Kaigala et al., 2008). Mendoza-Gallegos and colleagues outlined a resistive heating-based, low-cost and portable thermocycler, utilizing a copper-sheathed 50  $\Omega$  power resistor and a cooling fan (Mendoza-Gallegos et al., 2018). Lee and colleagues at the University of California Berkeley demonstrated an external heater-based ultrafast microfluidic PCR (Lee et al., 2019). Bubble generation reagent evaporation are the major drawbacks of microfluidic PCR, and to overcome the problems, a thin, impermeable polyethylene (PE) top layer was embedded into the microfluidic PCR chip to prevent vertical mass transport (Fig. 8c). Consequently, ultrafast microfluidic PCR amplification was completed in less than 3 min under bubble-free conditions.

## 5. Future directions and remaining challenges for next-generation NAAT

As previously outlined, several multidisciplinary approaches have fabricated and implemented various probes and diagnostic platforms in the molecular diagnostic field. To provide clinically useful diagnostic tools, NA amplification steps ideally need to proceed in a predictable

manner and to provide real-time quantitative profiles from which the concentration of target DNA can be determined. Analytical performances of the methods, including sensitivity, specificity and multiplex capability, should be tailored to the initial sample volume, target analyte concentration and sample sources to ensure the diagnostic reliability. Several challenges to engineer the next-generation NAATs still remain in terms of accommodating these requirements.

### 5.1. Tolerance to inhibitors and fidelity of DNA polymerase

High tolerance to NAAT inhibitors and great DNA polymerase fidelity denotes the ability to accurately replicate sequences, which is important factors for reliable molecular diagnoses (Mattila et al., 1991; Tindall and Kunkel, 1988). In principle, NAATs can be negatively impacted by several different inhibitors that are inherent to unprocessed clinical matrices (Schrader et al., 2012). The diagnostic performance of various NA amplification strategies is thus dependent on the origin of the sample - blood, urine, sputum or mucous swabs. Previously identified or potential inhibitors include heme, immunoglobulin G, lactoferrin, heparin, urea and polysaccharides (Sidstedt et al., 2018). Strategies to overcome the NAAT inhibition include the presence of PCR enhancers in the PCR fluid, as well as the high-level sample preparation. For example, bovine serum albumin, betaine or proteinase inhibitors have been widely used to reduce NAAT inhibition (Hall et al., 2013). NPs can also be utilized as additives to enhance polymerase tolerance and fidelity (Shen et al., 2009; Yang et al., 2008). Carbon materials, including single- and multi-walled carbon nanotubes and graphene, have also been reported as excellent nano-additive PCR enhancers (Yuce et al., 2014). Li et al. found that the addition of AuNP as



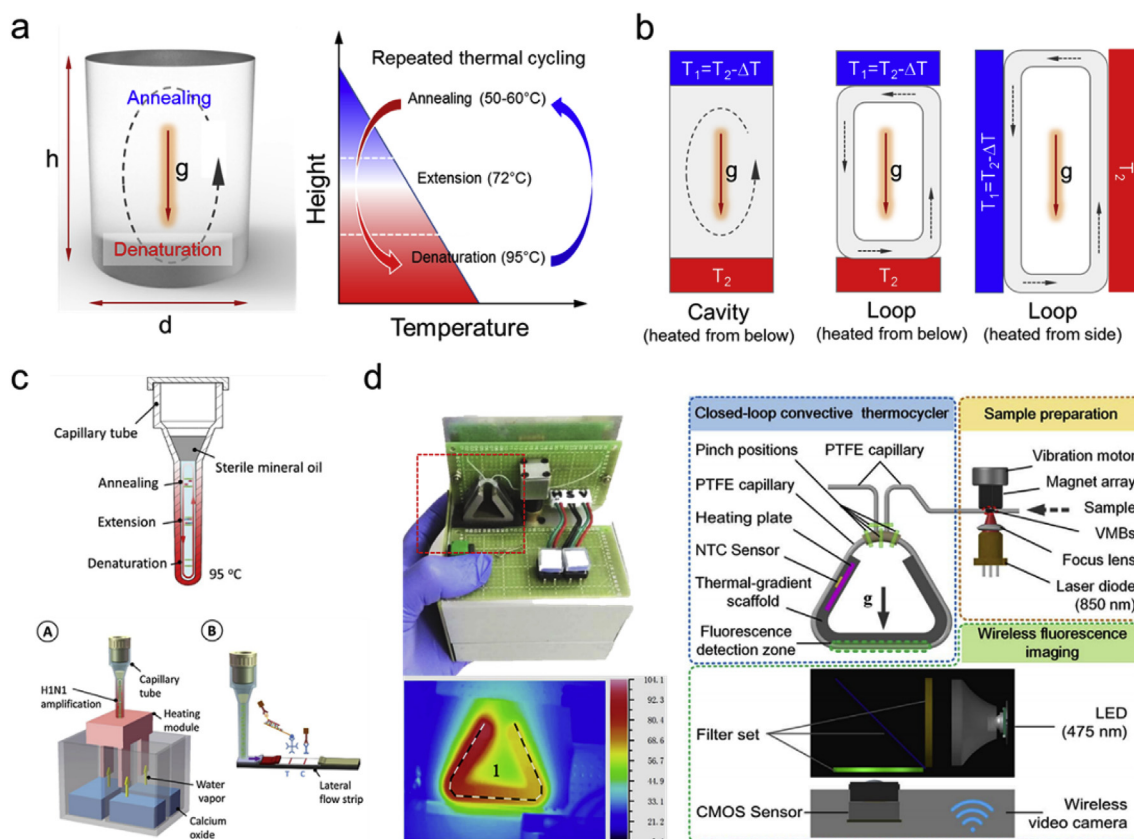


**Fig. 7.** Buoyancy-driven convective PCR. (a) Schematic illustration of the thermal convection in a cylindrical reactor. When the fixed temperature at the bottom is maintained higher than the top, a circulatory flow via a vertical density gradient can be generated in the enclosed fluid. For PCR thermocycling, the top and the bottom surfaces are sustained at the annealing and denaturing temperature, respectively. (b) Various reactor geometries with circulatory flow pattern. (c) Capillary tube design for convective PCR thermocycling (top). Instrument-free molecular diagnostic approach by calcium oxide mixture and lateral flow detection. Heat can be generated as calcium oxide interacts with water (bottom). Reprinted with permission from (Qiu et al., 2017a). Copyright 2017, Elsevier. (d) Integrated real-time convective PCR platform. Photograph of the integrated convective PCR system (90x95x125 mm) and infrared (IR) image of the triangular PCR scaffold (left). Convective PCR thermocycler assembly constructed with a magnetic bead-assisted photo-thermolysis module for sample preparation, closed-loop PCR tubing reactor and complementary metal-oxide-semiconductor (CMOS)-based real-time fluorescence detector (right). Reprinted with permission from (Shu et al., 2017). Copyright 2017, Elsevier.

an additive could result in 10,000-fold increase in the PCR detection sensitivity due to excellent heat transfer properties of the metal NPs (Li et al., 2005). Furthermore, isothermal amplification has been shown to be tolerant to many NAAT inhibitors, potentially reducing the procedural complexity of the extraction and purification stages of sample preparation (Kaneko et al., 2007; Nixon et al., 2014).

## 5.2. Bioanalytical methods with mobile-healthcare technology

Early NAATs were a qualitative test that could assess the presence or absence of genetic variations from the results of agarose gel electrophoresis. In the current diagnostic format, fluorescence detectors have been incorporated into a thermocycler to reveal amplification kinetics in real-time. The advancements decreased the time needed to reach a clinical decision, helping clinicians to explore wider differential diagnoses (Maurer, 2011). For example, the melting curve analysis has been widely applied to each amplicon for a better validation of the NAATs and to distinguish the true target amplicon from any spurious amplifications of unrelated targets (Eyigor et al., 2002).

Beyond these analytical methods, several other molecular diagnostics have evolved for mobile healthcare (m-healthcare). The m-healthcare technology is based on seamless connectivity, portability and robust functionality, and is gaining significant attention to bridge the existing gap between patients and clinicians. For instance, the Prakash group at Stanford University has shown a cost-effective, paper-

based microscope, called a 'Foldscope', for POCT applications (Cybulski et al., 2014). The Foldscope is an origami-based optical microscope that can be assembled within 10 min from a flat sheet of paper (Fig. 9a). The Foldscope includes ball lenses (BK7), a polymer aperture, LED and polypropylene filters to capture bright-field, dark-field and fluorescence images. The LED used in the Foldscope consumes only 6 mW of electrical power and can operate for over 50 h with a 3 V cell battery. The approach has significant benefits in scenarios dealing with highly contagious diseases, where the 'use-and-throw' concept of a disposable microscope could be of benefit for infectious disease control. As shown in Fig. 9b, various types of portable smartphone-based diagnostics platforms have been described (e.g., Lab-on-a-drone) which could monitor various physical and molecular activities (D'Ambrosio et al., 2015; Priye et al., 2016). In particular, the Ozcan group at UCLA has described a variety of portable microscopy options, enabling smartphone-based clinical diagnostics (Greenbaum et al., 2014; Joh et al., 2017; Kühnemund et al., 2017; Wei et al., 2013).

## 5.3. Artificial intelligence for biomedical analysis

Artificial intelligence (AI), including deep or machine learning, has great potential to achieve excellent diagnostic accuracy by reducing the human error and by guiding the diagnosis and prognosis of life-threatening diseases (Khan et al., 2001; Litjens et al., 2016; Palma et al., 2018). The advances in computational approaches have allowed

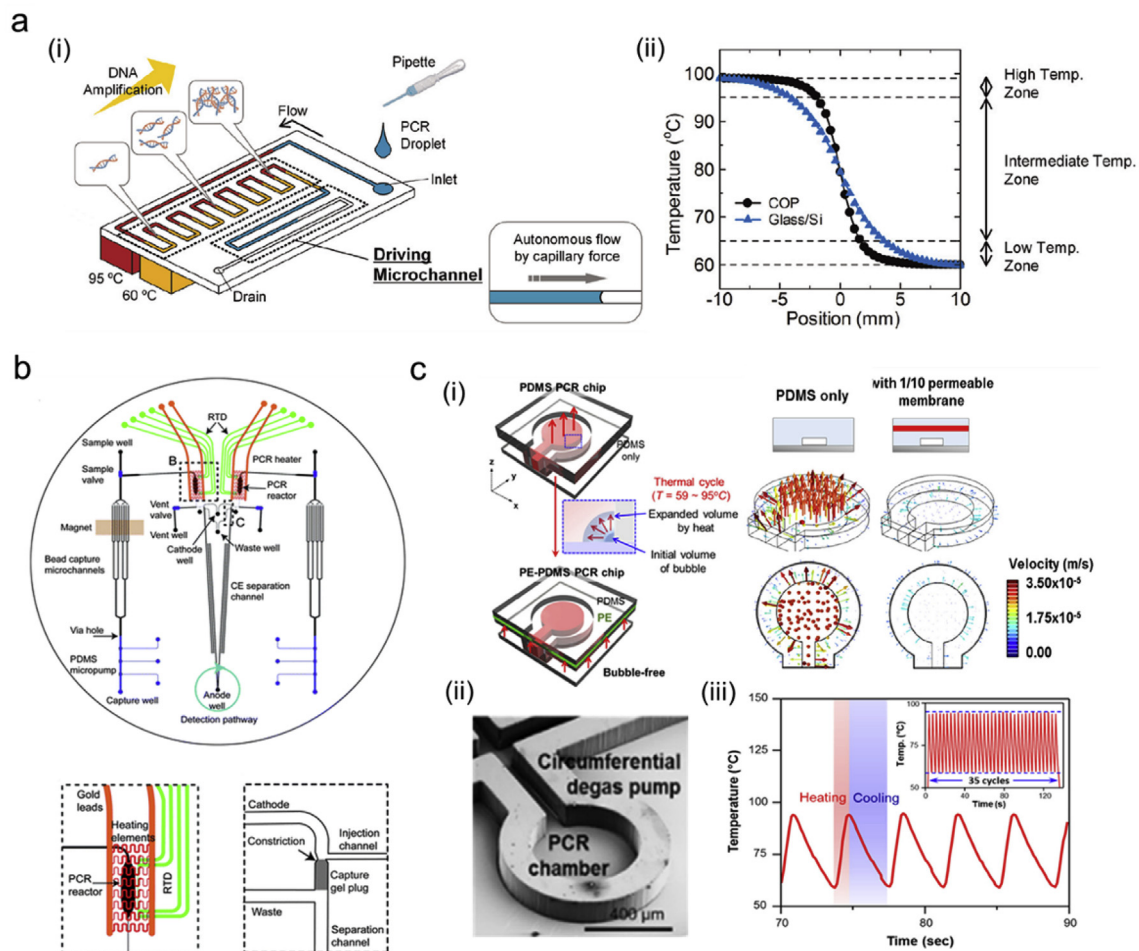


**Fig. 8.** Representative resistive heating methods. (a) Working principle of continuous-flow PCR. The PCR chip is placed on two heating blocks kept at 95°C and 60°C, respectively (left). Simulated temperature distribution in the plastic substrate (cyclo-olefin polymer, COP) and glass/Si. Reprinted with permission from (Tachibana et al., 2015). Copyright 2015, Elsevier. (b) Schematic illustration of fully integrated microdevice. The resistive heater and resistance temperature detector (RTD) were fabricated from the same substrate. The bottom left image shows the expanded description of the PCR chamber, microheater and RTD. Reprinted with permission from (Liu et al., 2011). Copyright 2011, Royal Chemical Society. (c) Bubble-free ultrafast microfluidic PCR approach. To prevent the evaporation of PCR fluids by liquid/gas diffusion, an impermeable polymer layer was embedded into the microfluidic PCR chip. The ultrafast PCR test was completed in less than 3 min using external heating blocks. Reprinted with permission from (Lee et al., 2019). Copyright 2019, Elsevier.

researchers to (i) facilitate biomarker discovery; (ii) enhance diagnostic accuracy and risk assessment; and (iii) provide better therapeutic options (Göröcs et al., 2018; Oustimov and Vu, 2014; Sherafatian, 2018; Sherafatian (2018)). A team from Harvard Medical School noticed a 2.9% error rate in the AI model of breast cancer diagnosis from biopsy slide images (Wang et al., 2016). However, pairing the deep learning with pathologist's inputs showed a significantly lower error rate at 0.5%. Deep learning has also been applied in the molecular diagnostics. As shown in Fig. 9c and d, deep- or machine-learning was used for the sequence specificity prediction via the 'DeepBind' training tool as well as for the diagnosis of pancreatic cancer from circulating exosomes (Alipanahi et al., 2015; Ko et al., 2017). In another example, the 'DeepGene' classifier, based on a somatic point mutation based cancer classification (SMCC), was developed to predict cancer types/subtypes and their point mutations (Yuan et al., 2016). In this study, a deep learning model was applied to extract dataset features between combinatorial point mutations and cancer types. Similarly, a deep learning approach was used to identify enriched genes from RNA-seq expression data to diagnose breast cancer (Danaee et al., 2017). The researchers used a stacked denoising autoencoder (SDAE) algorithm to extract features and to implement a supervised classification model to evaluate and verify those features against cancer detection.

## 6. Conclusion

Over the last decade, limitations of the conventional PCR approaches have become more apparent including large reaction volumes, the lengthy run times from time-consuming thermal cycling requirements. Although NAATs are highly sensitive and specific, they still are subject to a number of challenges such as the delays in response time, originating from the amplification step, when compared to the nano-material-based NA testing. A number of alternative NA amplification methods, instruments and novel approaches have been proposed to build fast and convenient PCR devices for POCT. Recently, one major demand for new PCR devices has been on the excellent analytical performance, which includes ultrafast run time with high sensitivity and specificity, compatible with instant clinical decision-making. Another important factor is their ease of use, and this can be achieved by an integrated sample-to-answer processing of samples (e.g., as a stand-alone operation) and by a simple operation protocol of NAAT that can be followed by all clinical staff, meeting the eligible criteria for the Clinical Laboratory Improvement Amendments (CLIA)-waived status. Increasing importance will be given to innovative, ultrafast amplification methods and tools which combined with AI-associated data analysis processes (i.e., electronic decision-making algorithms and e-learning systems) and mobile-healthcare networks. The ultrafast PCR

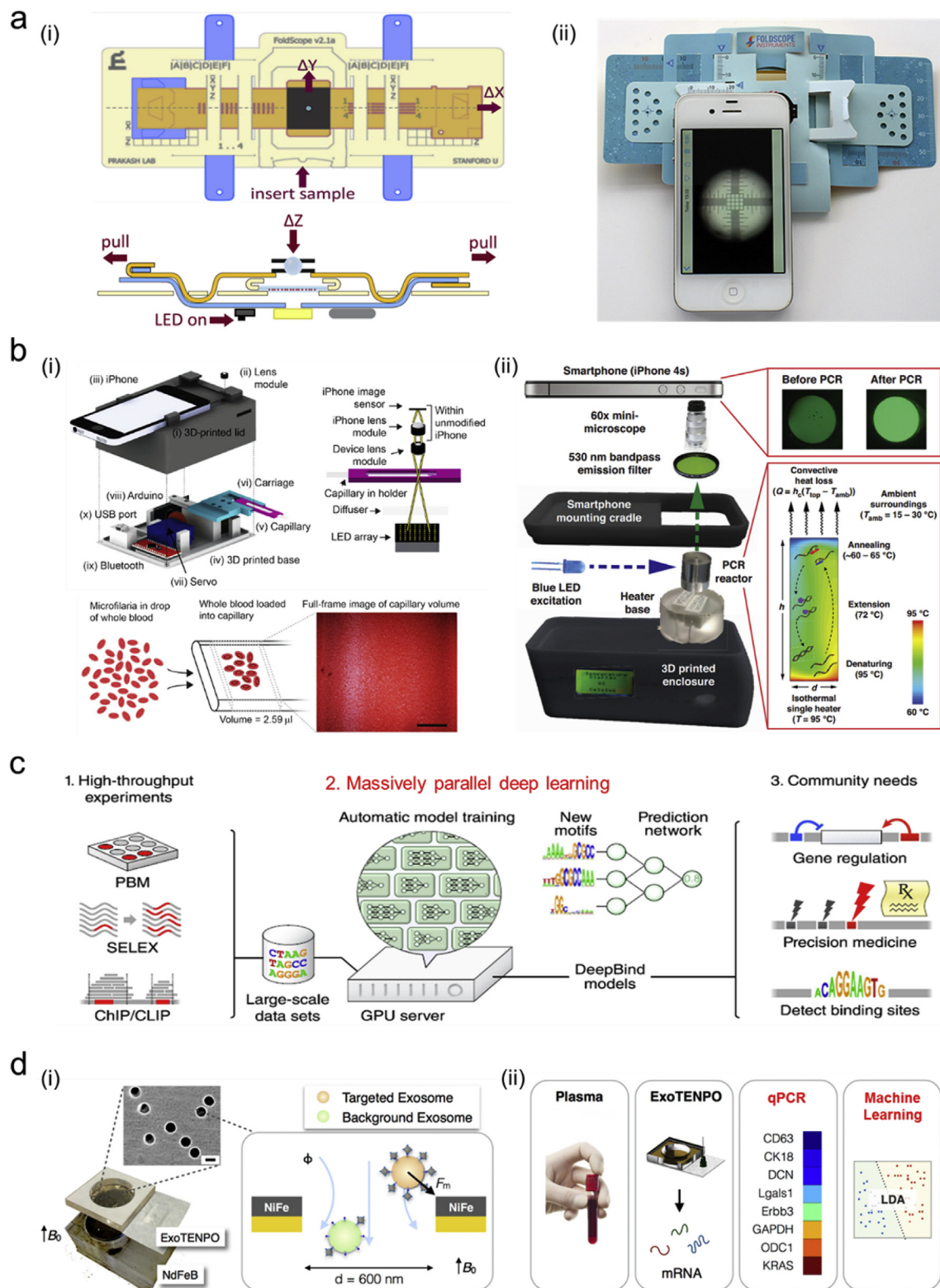


**Fig. 9.** Portable detection systems and artificial intelligence-based diagnostic approaches. (a) Low-cost Foldscope. CAD layout and cross-sectional view of Foldscope paper components (i), demonstration of the Foldscope (ii). (b) Automated cell phone-based video microscope (left). Lab-on-a-drone components. A device using a smartphone camera was used for fluorescence detection of PCR amplicon (right). (c) DeepBind input data, training procedure and applications. The sequence specificities of DNA- and RNA-binding proteins can be measured by various experimental techniques. DeepBind is then used with the data to train high-quality models. (d) ExoTENPO-based exosome diagnostics. A photograph of ExoTENPO (right) for exosome analysis and a machine learning algorithm-based pancreatic cancer diagnosis. Figures a, b (left), b (right), c, and d reprinted with permission from (Alipanahi et al., 2015; Cybulski et al., 2014; D'Ambrosio et al., 2015; Ko et al., 2017; Priye et al., 2016), respectively.



with sample-to-answer and time-sensitive platforms are well suited to various end users, providing the ability to cater to patients in both wealthy and resource-limited countries. As such, these new approaches have a great potential to lead more innovations in next-generation molecular diagnostics using POCT platforms.

## Declaration of interests

The authors declare that they have no known competing financial interests or personal relationships that could have appeared to influence the work reported in this paper.

## CRediT authorship contribution statement

**Sang Hun Lee:** Conceptualization, Data curation, Writing - original draft. **Seung-min Park:** Supervision, Validation, Visualization, Writing - review & editing. **Brian N. Kim:** Supervision, Validation, Visualization, Writing - review & editing. **Oh Seok Kwon:** Supervision, Validation, Visualization, Writing - review & editing. **Won-Yep Rho:** Supervision, Validation, Visualization, Writing - review & editing. **Bong-Hyun Jun:** Conceptualization, Data curation, Writing - original draft.

## Acknowledgements

This research was supported by the Bio and Medical Technology Development Program of the National Research Foundation (NRF) funded by the Korean government (MSIP & MOHW; grant no. 2016M3A9B6918892) and funded by the Korean Health Technology R & D Project, Ministry of Health & Welfare (HI17C1264). Also, this research was supported by the National Research Foundation of Korea (NRF) Grant funded by the Ministry of Science and ICT for First-Mover Program for Accelerating Disruptive Technology Development (NRF-2018M3C1B9069834) and the KRIBB Initiative Research Program.

## References

- Agrawal, N., Ugaz, V.M., 2007. A buoyancy-driven compact thermocycler for rapid PCR. *Clin. Lab. Med.* 27, 215–223.
- Agrawal, N., Hassan, Y.A., Ugaz, V.M., 2007. A pocket-sized convective PCR thermocycler. *Angew. Chem.* 46, 4316–4319.
- Alipanahi, B., Delong, A., Weirauch, M.T., Frey, B.J., 2015. Predicting the sequence specificities of DNA- and RNA-binding proteins by deep learning. *Nat. Biotechnol.* 33, 831–838.
- Arvidsson, S., Kwasniewski, M., RiañoPachón, D.M., Mueller-Roeber, B., 2008. QuantPrime – a flexible tool for reliable high-throughput primer design for quantitative PCR. *BMC Bioinf.* 9, 465.
- Arya, M., Shergill, I.S., Williamson, M., Gommersall, L., Arya, N., Patel, H.R., 2005. Basic principles of real-time quantitative PCR. *Expert Rev. Mol. Diagn.* 5, 209–219.
- Asiello, P.J., Baeumner, A.J., 2011. Miniaturized isothermal nucleic acid amplification, a review. *Lab Chip* 11, 1420–1430.
- Ballard, Z., Ozcan, A., 2018. Nucleic acid quantification in the field. *Nat. Biomed. Eng.* 2, 629–630.
- Bartsch, M.S., Edwards, H.S., Lee, D., Moseley, C.E., Tew, K.E., Renzi, R.F., Vreugde, J.L.V.d., Kim, H., Knight, D.L., Sinha, A., Branda, S.S., Patel, K.D., 2015. The rotary zone thermal cycler: a low-power system enabling automated rapid PCR. *PLoS One* 10, e0118182.
- Bhambhani, M.S., Benson, B., Chai, C., Katsikis, G., Johri, A., Prakash, M., 2017. Hand-powered ultralow-cost paper centrifuge. *Nat. Biomed. Eng.* 1, 0009.
- Bi, S., Yue, S., Zhang, S., 2017. Hybridization chain reaction: a versatile molecular tool for biosensing, bioimaging, and biomedicine. *Chem. Soc. Rev.* 46, 4281–4298.
- Bradshaw, S.M., Wyk, E.J.v., Swardt, J.B.d., 1998. Microwave heating principles and the application to the regeneration of granular activated carbon. *J. South. Afr. Inst. Min. Metall.* 201–2011.
- Burger, J., Gross, A., Mark, D., Stetten, F.v., Zengerle, R., Roth, G., 2011. IR thermocycler for centrifugal microfluidic platform with direct on-disk wireless temperature measurement system. In: 16th International Solid-State Sensors, Actuators and Microsystems Conference Th2A. 006. pp. 2867–2870.
- Cao, L., Cui, X., Hu, J., Li, Z., Choi, J.R., Yang, Q., Lin, M., Huili, Y., Xu, F., 2017. Advances in digital polymerase chain reaction (dPCR) and its emerging biomedical applications. *Biosens. Bioelectron.* 90, 459–474.
- Chen, X., Song, L., Assadsangabi, B., Fang, J., Ali, M.S.M., Takahata, K., 2013. Wirelessly addressable heater array for centrifugal microfluidics and escherichia coli sterilization. *Conf. Proc. IEEE Eng. Med. Biol. Soc.* 5505–5508.
- Chen, J.S., Ma, E., Harrington, L.B., Costa, M.D., Tian, X., Palefsky, J.M., Doudna, J.A., 2018. CRISPR-Cas12a target binding unleashes indiscriminate single-stranded DNase activity. *Science* 360, 436–439.
- Cheng, Y., Wang, Y., Wang, Z., Huang, L., Bi, M., Xu, W., Wang, W., Ye, X., 2017. A mechanical cell disruption microfluidic platform based on an on-chip micropump. *Biomicrofluidics* 11, 024112.
- Chertow, D.S., 2018. Next-generation diagnostics with CRISPR. *Science* 360, 381–382.
- Chiappin, S., Antonelli, G., Gatti, R., Palo, E.F.D., 2007. Saliva specimen: a new laboratory tool for diagnostic and basic investigation. *Clin. Chim. Acta* 383, 30–40.
- Compton, J., 1991. Nucleic acid sequence-based amplification. *Nature* 350, 91–92.
- Craw, P., Balachandran, W., 2012. Isothermal nucleic acid amplification technologies for point-of-care diagnostics: a critical review. *Lab Chip* 12, 2469–2486.
- Cybulski, J.S., Clements, J., Prakash, M., 2014. Foldscape: origami-based paper microscope. *PLoS One* 9, e98781.
- Danaee, P., Ghaeini, R., Hendrix, D.A., 2017. A deep learning approach for cancer detection and relevant gene identification. *Pac. Symp. Biocomput.* 22, 219–229.
- Dean, F.B., Hosono, S., Fang, L., Wu, X., Faruqi, A.F., Bray-Ward, P., Sun, Z., Du, Q.Z.Y., Du, J., Driscoll, M., Song, W., Kingsmore, S.F., Egholm, M., Lasken, R.S., 2002. Comprehensive human genome amplification using multiple displacement amplification. *Proc. Natl. Acad. Sci.* 99, 5261–5266.
- Didenko, V.V., 2001. DNA probes using fluorescence resonance energy transfer (FRET): designs and applications. *Biotechniques* 31, 1106–1121.
- Dimov, I.K., Garcia-Cordero, J.L., O'Grady, J., Poulsen, C.R., Viguier, C., Kent, L., Daly, P., Lincoln, B., Maher, M., O'Kennedy, R., Smith, T.J., Ricco, A.J., Lee, L.P., 2008. Integrated microfluidic tmRNA purification and real-time NASBA device for molecular diagnostics. *Lab Chip* 8, 2071–2078.
- Ding, X., Mu, Y., 2016. Digital Nucleic Acid Detection Based on Microfluidic Lab-On-A-Chip Devices. *InTech*, pp. 125–155.
- Dirks, R.M., Pierce, N.A., 2004. Triggered amplification by hybridization chain reaction. *Proc. Natl. Acad. Sci.* 101, 15275–15278.
- D'Ambrosio, M.V., Bakalar, M., Bennuru, S., Reber, C., Skandarajah, A., Nilsson, L., Switz, N., Kamgno, J., Pion, S., Boussinesq, M., Nutman, T.B., Fletcher, D.A., 2015. Point-of-care quantification of blood-borne filarial parasites with a mobile phone microscope. *Sci. Transl. Med.* 7, 286re284.
- Easley, C.J., Karlinsky, J.M., Landers, J.P., 2006. On-chip pressure injection for integration of infrared-mediated DNA amplification with electrophoretic separation. *Lab Chip* 6, 601–610.
- Erickson, D., Sinton, D., Li, D., 2003. Joule heating and heat transfer in poly(dimethylsiloxane) microfluidic systems. *Lab Chip* 3, 141–149.
- Evanko, D., 2004. Hybridization chain reaction. *Nat. Methods* 1, 186–187.
- Eyigor, A., Carli, K.T., Unal, C.B., 2002. Implementation of real-time PCR to tetrathionate broth enrichment step of Salmonella detection in poultry. *Lett. Appl. Microbiol.* 34, 37–41.
- Farrar, J.S., Wittwer, C.T., 2015. Extreme PCR: efficient and specific DNA amplification in 15–60 seconds. *Clin. Chem.* 61, 145–154.
- Gao, Z., Qiu, Z., Lu, M., Shu, J., Tang, D., 2017. Hybridization chain reaction-based colorimetric aptasensor of adenosine 5'-triphosphate on unmodified gold nanoparticles and two label-free hairpin probes. *Biosens. Bioelectron.* 89, 1006–1012.
- Garg, P., Hella, M., Borca-Tasiuc, D.-A., Mohamed, H., 2008. DNA amplification by PCR using low cost, programmable microwave heating. *TechConnect. Briefs.* 2, 577–580.
- Gill, P., Ghaemi, A., 2008. Nucleic acid isothermal amplification technologies Nucleos. *Nucleot. Nucl.* 27, 224–243.
- GNA Biosolutions GmbH, G. <https://www.gna-bio.com/>.
- Gootenberg, J.S., Abudayyeh, O.O., Kellner, M.J., Joung, J., Collins, J.J., Zhang, F., 2018. Multiplexed and portable nucleic acid detection platform with Cas13, Cas12a, and Csm6. *Science* 360, 439–444.
- Greenbaum, A., Zhang, Y., Feizi, A., Chung, P.-L., Luo, W., Kandukuri, S.R., Ozcan, A., 2014. Wide-field computational imaging of pathology slides using lens-free on-chip microscopy. *Sci. Transl. Med.* 6, 267ra175.
- Gu, L., Yan, W., Liu, L., Wang, S., Zhang, X., Lyu, M., 2018. Research progress on rolling circle amplification (RCA)-Based biomedical sensing. *Pharmaceuticals* 11, E35.
- Gulliksen, A., Solli, L.A., Drese, K.S., Sörensen, O., Karlsen, F., Rogne, H., Hovig, E., Sirevåg, R., 2005. Parallel nanoliter detection of cancer markers using polymer microchips. *Lab Chip* 5, 416–420.
- Göröcs, Z., Tamamitsu, M., Bianco, V., Wolf, P., Roy, S., Shindo, K., Yanny, K., Wu, Y., Koydemir, H.C., Rivenon, Y., Ozcan, A., 2018. A deep learning-enabled portable imaging flow cytometer for cost-effective, high-throughput, and label-free analysis of natural water samples. *Light Sci. Appl.* 7, 66.
- Hahn, E., Cha, M.G., Kang, E.J., Pham, X.-H., Lee, S.H., Kim, H.-M., Kim, D.-E., Lee, Y.-S., Jeong, D.H., Jun, B.-H., 2018. Multi-layer Ag-embedded silica nanostructure as SERS-based chemical sensor with dual-function internal standards. *ACS Appl. Mater. Interfaces* 10, 40748–40755.
- Hall, A.T., Zovanyi, A.M., Christensen, D.R., Koehler, J.W., Minogue, T.D., 2013. Evaluation of inhibitor-resistant real-time PCR methods for diagnostics in clinical and environmental samples. *PLoS One* 8, e73845.
- Heginbotham, M.L., Magee, J.T., Flanagan, P.G., 2003. Evaluation of the Idaho technology LightCycler™ PCR for the direct detection of mycobacterium tuberculosis in respiratory specimens. *Int. J. Tuberc. Lung Dis.* 7, 78–83.
- Herold, K.E., Sergeev, N., Matviyenko, A., Rasooly, A., 2009. Rapid DNA amplification using a battery-powered thin-film resistive thermocycler. *Methods Mol. Biol.* 504, 441–458.
- Holland, P.M., Abramson, R.D., Watson, R., Gelfand, D.H., 1991. Detection of specific polymerase chain reaction product by utilizing the 5'-3' exonuclease activity of *Thermus aquaticus* DNA polymerase. *Proc. Natl. Acad. Sci.* 88, 7276–7280.
- Hou, T., Wang, X., Liu, X., Lu, T., Liu, S., Li, F., 2014. Amplified detection of T4 polynucleotide kinase activity by the coupled  $\lambda$  exonuclease cleavage reaction and

- catalytic assembly of bimolecular beacons. *Anal. Chem.* 86, 884–890.
- Islam, M.S., Aryasomayajula, A., Selvaganapathy, P.R., 2017. A review on macroscale and microscale cell lysis methods. *Micromachines* 8, 83.
- Jiang, L., Mancuso, M., Lu, Z., Akar, G., Cesarman, E., Erickson, D., 2014. Solar thermal polymerase chain reaction for smartphone-assisted molecular diagnostics. *Sci. Rep.* 4, 4137.
- Joh, D.Y., Hucknall, A.M., Wei, Q., Mason, K.A., Lund, M.L., Fontes, C.M., Hill, R.T., Blair, R., Zimmers, Z., Achar, R.K., Tseng, D., Gordan, R., Freemark, M., Ozcan, A., Chilukoti, A., 2017. Inkjet-printed point-of-care immunoassay on a nanoscale polymer brush enables subpicomolar detection of analytes in blood. *Proc. Natl. Acad. Sci.* 114, E7054–E7062.
- Kaigala, G.V., Hoang, V.N., Stickel, A., Lauzon, J., Manage, D., Pilarski, L.M., Backhouse, C.J., 2008. An inexpensive and portable microchip-based platform for integrated RT-PCR and capillary electrophoresis. *Analyst* 133, 331–338.
- Kaneko, H., Kawana, T., Fukushima, E., Suzutani, T., 2007. Tolerance of loop-mediated isothermal amplification to a culture medium and biological substances. *J. Biochem. Biophys. Methods* 70, 499–501.
- Khan, J., Wei, J.S., Ringnér, M., Saal, L.H., Ladanyi, M., Westermann, F., Berthold, F., Schwab, M., Antonescu, C.R., Peterson, C., Meltzer, P.S., 2001. Classification and diagnostic prediction of cancers using gene expression profiling and artificial neural networks. *Nat. Med.* 7, 673–679.
- Kim, J.A., Lee, J.Y., Seong, S., Cha, S.H., Lee, S.H., Kim, J.J., Park, T.H., 2006. Fabrication and characterization of a PDMS-glass hybrid continuous-flow PCR chip. *Biochem. Eng. J.* 29, 91–97.
- Kim, J.A., Lee, S.H., Park, H., Kim, J.H., Park, T.H., 2010. Microheater based on magnetic nanoparticle embedded PDMS. *Nanotechnology* 21, 165102.
- Ko, J., Bhagwat, N., Yee, S.S., Ortiz, N., Sahmoud, A., Black, T., Aiello, N.M., McKenzie, L., O'Hara, M., Redlinger, C., Romeo, J., Carpenter, E.L., Stanger, B.Z., Issadore, D., 2017. Combining machine learning and nanofluidic technology to diagnose pancreatic cancer using exosomes. *ACS Nano* 11, 11182–11193.
- Kopp, M.U., Mello, A.J.D., Manz, A., 1998. Chemical amplification: continuous-flow PCR on a chip. *Science* 280, 1046–1048.
- Kühnemund, M., Wei, Q., Darai, E., Wang, Y., Hernández-Neuta, I., Yang, Z., Tseng, D., Ahlford, A., Mathot, L., Sjöblom, T., Ozcan, A., Nilsson, M., 2017. Targeted DNA sequencing and in situ mutation analysis using mobile phone microscopy. *Nat. Commun.* 8, 13913.
- Kumar, S., Kumar, A., Venkatesan, G., 2018. Isothermal nucleic acid amplification system: an update on methods and applications. *J. Genet. Genom.* 2, 112.
- Lee, S.H., Jun, B.-H., 2019. Advances in dynamic microphysiological organ-on-a-chip: design principle and its biomedical application. *J. Ing. Eng. Chem.* 71, 725–733.
- Lee, H.J., Kim, J.-H., Lim, H.K., Cho, E.C., Huh, N., Ko, C., Park, J.C., Choi, J.-W., Lee, S.S., 2010. Electrochemical cell lysis device for DNA extraction. *Lab Chip* 10, 626–633.
- Lee, S.H., Kwon, O.S., Song, H.S., Park, S.J., Sung, J.H., Jang, J., Park, T.H., 2012a. Mimicking the human smell sensing mechanism with an artificial nose platform. *Biomaterials* 33, 1722–1729.
- Lee, S.H., Sung, J.H., Park, T.H., 2012b. Nanomaterial-based biosensor as an emerging tool for biomedical applications. *Ann. Biomed. Eng.* 40, 1384–1397.
- Lee, J.-H., Cheglakov, Z., Yi, J., Cronin, T.M., Gibson, K.J., Tian, B., Weizmann, Y., 2017. Plasmonic photothermal gold bipyramid nanoreactors for ultrafast real-time biosays. *J. Am. Chem. Soc.* 139, 8054–8057.
- Lee, S.H., Hong, S., Song, J., Cho, B., Han, E.J., Kondapavulur, S., Kim, D., Lee, L.P., 2018. Microphysiological analysis platform of pancreatic islet  $\beta$ -cell spheroids. *Adv. Healthc. Mater.* 7, 1701111.
- Lee, S.H., Song, J., Cho, B., Hong, S., Hoxha, O., Kang, T., Kim, D., Lee, L.P., 2019. Bubble-free rapid microfluidic PCR. *Biosens. Bioelectron.* 126, 725–733.
- Li, M., Lin, Y.-C., Wu, C.-C., Liu, H.-S., 2005. Enhancing the efficiency of a PCR using gold nanoparticles. *Nucleic Acids Res.* 33, e184.
- Li, L., Feng, J., Liu, H., Li, Q., Tong, L., Tang, B., 2016a. Two-color imaging of microRNA with enzyme-free signal amplification via hybridization chain reactions in living cells. *Chem. Sci.* 7, 1940–1945.
- Li, T.-J., Chang, C.-M., Chang, P.-Y., Chuang, Y.-C., Huang, C.-C., Su, W.-C., Shieh, D.-B., 2016b. Handheld energy-efficient magnetooptical real-time quantitative PCR device for target DNA enrichment and quantification. *NPG Asia Mater.* 8, e277.
- Liew, M., Pryor, R., Palais, R., Meadows, C., Erali, M., Lyon, E., Wittwer, C., 2004. Genotyping of single-nucleotide polymorphisms by high-resolution melting of small amplicons. *Clin. Chem.* 50, 1156–1164.
- Liong, M., Hoang, A.N., Chung, J., Gural, N., Ford, C.B., Min, C., Shah, R.R., Ahmad, R., Fernandez-Suarez, M., Fortune, S.M., Toner, M., Lee, H., Weissleder, R., 2013. Magnetic barcode assay for genetic detection of pathogens. *Nat. Commun.* 4, 1752.
- Litjens, G., Sánchez, C.I., Timofeeva, N., Hermesen, M., Nagtegaal, I., Kovacs, I., Kaa, C.H.-v.d., Peter Bult, B.v.G., Laak, J.v.d., 2016. Deep learning as a tool for increased accuracy and efficiency of histopathological diagnosis. *Sci. Rep.* 6, 26286.
- Little, M.C., Andrews, J., Moore, R., Bustos, S., Jones, L., Embres, C., Durmowicz, G., Harris, J., Berger, D., Yanson, K., Rostkowski, C., Yursis, D., Price, J., Fort, T., Walters, A., Collis, M., Llorin, O., Wood, J., Failing, F., O'Keefe, C., Scrivens, B., Pope, B., Hansen, T., Marino, K., Williams, K., Boenisch, M., 1999. Strand displacement amplification and homogeneous real-time detection incorporated in a second-generation DNA probe system, BDProbeTecET. *Clin. Chem.* 45, 777–784.
- Liu, P., Li, X., Greenspoon, S.A., Scherer, J.R., Mathies, R.A., 2011. Integrated DNA purification, PCR, sample cleanup, and capillary electrophoresis microchip for forensic human identification. *Lab Chip* 11, 1041–1048.
- Liu, X., Chen, M., Hou, T., Wang, X., Liu, S., Li, F., 2014. Label-free colorimetric assay for base excision repair enzyme activity based on nicking enzyme assisted signal amplification. *Biosens. Bioelectron.* 54, 598–602.
- Lizardi, P.M., Huang, X., Zhu, Z., Bray-Ward, P., Thomas, D.C., Ward, D.C., 1998. Mutation detection and single-molecule counting using isothermal rolling-circle amplification. *Nat. Genet.* 19, 225–232.
- Malamud, D., Rodriguez-Chavez, I.R., 2011. Saliva as a diagnostic fluid. *Dent. Clin. N. Am.* 55, 159–178.
- Maltezos, G., Johnston, M., Taganov, K., Srichantaratsamee, C., Gorman, H., Baltimore, D., Chantratita, W., Scherer, A., 2010. Exploring the limits of ultrafast polymerase chain reaction using liquid for thermal heat exchange: a proof of principle. *Appl. Phys. Lett.* 97, 264101.
- Marchiarullo, D.J., Sklavounos, A.H., Oh, K., Poe, B.L., Barker, N.S., Landers, J.P., 2013. Low-power microwave-mediated heating for microchip-based PCR. *Lab Chip* 13, 3417–3425.
- Marx, V., 2015. PCR heads into the field. *Nat. Methods* 12, 393–397.
- Mattila, P., Korpela, J., Tenkanen, T., Pitkämä, K., 1991. Fidelity of DNA synthesis by the *Thermococcus litoralis* DNA polymerase—an extremely heat stable enzyme with proofreading activity. *Nucleic Acids Res.* 19, 4967–4973.
- Maurer, J.J., 2011. Rapid detection and limitations of molecular techniques. *Annu. Rev. Food Sci. Technol.* 2, 259–279.
- Mendoza-Gallegos, R.A., Rios, A., Garcia-Cordero, J.L., 2018. An affordable and portable thermocycler for real-time PCR made of 3d-printed parts and off-the-shelf electronics. *Anal. Chem.* 90, 5563–5568.
- Mhlanga, M.M., Tyagi, S., 2006. Using tRNA-linked molecular beacons to image cytoplasmic mRNAs in live cells. *Nat. Protoc.* 1, 1392–1398.
- Mhlanga, M.M., Vargas, D.Y., Fung, C.W., Kramer, F.R., Tyagi, S., 2005. tRNA-linked molecular beacons for imaging mRNAs in the cytoplasm of living cells. *Nucleic Acids Res.* 33, 1902–1912.
- Mielczarek, W.S., Obaje, E.A., Bachmann, T.T., Kersaudy-Kerhoas, M., 2016. Microfluidic blood plasma separation for medical diagnostics: is it worth it? *Lab Chip* 16, 3441–3448.
- Miralles, V., Huerre, A., Malloggi, F., Jullien, M.-C., 2013. A review of heating and temperature control in microfluidic systems: techniques and applications. *Diagnostics* 3, 33–67.
- Muddu, R., Hassan, Y.A., Ugaz, v.M., 2011. Rapid PCR thermocycling using microscale thermal convection. *J. Vis. Exp.* 49, 2366.
- Mulberry, G., White, K.A., Vaidya, M., Sugaya, K., Kim, B.N., 2017. 3D printing and milling a real-time PCR device for infectious disease diagnostics. *PLoS One* 12, e0179133.
- Mulberry, G., Vuillier, A., Vaidya, M., Sugaya, K., Kim, B.N., 2018. Handheld battery-operated sample preparation device for qPCR nucleic acid detections using simple contactless pouring. *Anal. Methods* 10, 4671–4679.
- Myhrvold, C., Freije, C.A., Gootenberg, J.S., Abudayyeh, O.O., Metsky, H.C., Durbin, A.F., Kellner, M.J., Tan, A.L., Paul, L.M., Parham, L.A., Garcia, K.F., Barnes, K.G., Chak, B., Mondini, A., Nogueira, M.L., Isern, S., Michael, S.F., Lorenzana, I., Yozwiak, N.L., MacInnis, B.L., Bosch, I., Gehrke, L., Zhang, F., Sabeti, P.C., 2018. Field-deployable viral diagnostics using CRISPR-Cas13. *Science* 360, 444–448.
- Navarro, J.R.G., Lerouge, F., Micouin, G., Cefruga, C., Favier, A., Charreyre, M.T., Blanchard, N.P., Lerne, J., Chaput, F., Focsan, M., Kamada, K., Baldeck, P.L., Parola, S., 2014. Plasmonic bipyramids for fluorescence enhancement and protection against photobleaching. *Nanoscale* 6, 5138–5145.
- Neuzil, P., Zhang, C., Pipper, J., Oh, S., Zhuo, L., 2006. Ultrafast miniaturized real-time PCR: 40 cycles in less than six minutes. *Nucleic Acids Res.* 34, e77.
- Nixon, G., Garson, J.A., Grant, P., Nastouli, E., Foy, C.A., Huggett, J.F., 2014. Comparative study of sensitivity, linearity, and resistance to inhibition of digital and nondigital polymerase chain reaction and loop mediated isothermal amplification assays for quantification of human cytomegalovirus. *Anal. Chem.* 86, 4387–4394.
- Notomi, T., Okayama, H., Masubuchi, H., Yonekawa, T., Watanabe, K., Amino, N., Hase, T., 2000. Loop-mediated isothermal amplification of DNA. *Nucleic Acids Res.* 28, E63.
- Notomi, T., Mori, Y., Tomita, N., Kanda, H., 2015. Loop-mediated isothermal amplification (LAMP): principle, features, and future prospects. *J. Microbiol.* 53, 1–5.
- Oda, R.P., Strausbauch, M.A., Huhmen, A.F.R., Borson, N., Jurens, S.R., Craighead, J., Wettstein, P.J., Eckloff, B., Kline, B., Landers, J.P., 1998. Infrared-mediated thermocycling for ultrafast polymerase chain reaction amplification of DNA. *Anal. Chem.* 70, 4361–4368.
- Orrling, K., Nilsson, P., Gullberg, M., Larhed, M., 2004. An efficient method to perform milliliter-scale PCR utilizing highly controlled microwave thermocycling. *Chem. Commun.* 0, 790–791.
- Oustimov, A., Vu, V., 2014. Artificial neural networks in the cancer genomics frontier. *Transl. Cancer Res.* 3, 191–201.
- Oyebanji, T., 2013. Evaluation of Cepheid SmartCycler and EuroClone duplicareal time dual easy CT assay for confirmation of Chlamydia trachomatis bioscience. *Horizons* 6, hzt005.
- Pal, Debjani, Venkataraman, V., 2002. A portable battery-operated chip thermocycler based on induction heating. *Sens. Actuator A-Phys.* 102, 151–156.
- Pal, D., Venkataraman, V., Mohan, K.N., Chandra, H.S., Natarajan, V., 2004. A power-efficient thermocycler based on induction heating for DNA amplification by polymerase chain reaction. *Rev. Sci. Instrum.* 75, 2880–2883.
- Palma, S.I.C.J., Tragudo, A.P., Porteira, A.R., Frias, M.J., Gamboa, H., Roque, A.C.A., 2018. Machine learning for the meta-analyses of microbial pathogens' volatile signatures. *Sci. Rep.* 8, 3360.
- Park, S.-M., Sabour, A.F., Son, J.H., Lee, S.H., Lee, L.P., 2014. Toward integrated molecular diagnostic system (iMDx): principles and applications. *IEEE Trans. Biomed. Eng.* 61, 1506–1521.
- Park, S.-m., Wong, D.J., Ooi, C.C., Kurtz, D.M., Vermesh, O., Aalipour, A., Suh, S., Pian, K.L., Chabon, J.J., Lee, S.H., Jamali, M., Say, C., Carter, J.N., Lee, L.P., Kuschner, W.G., Schwartz, E.J., Shrager, J.B., Neal, J.W., Wakelee, H.A., Diehn, M., Nair, V.S., Wang, S.X., Gambhir, S.S., 2016. Molecular profiling of single circulating tumor cells

- from lung cancer patients. *Proc. Natl. Acad. Sci.* 113, E8379–E8386.
- Park, S.-m., Aalipour, A., Vermesh, O., Yu, J.H., Gambhir, S., 2017. Towards clinically translatable in vivo nanodiagnostics. *Nat. Rev. Mater.* 2, 17014.
- Pavlov, A.R., Pavlova, N.V., Kozayavkin, S.A., Slesarev, A.I., 2004. Recent developments in the optimization of thermostable DNA polymerases for efficient applications. *Trends Biotechnol.* 22, 253–260.
- Pham, X.H., Baek, A., Kim, T.H., Lee, S.H., Rho, W.Y., Chung, W.J., Kim, D.E., Jun, B.H., 2017. Graphene oxide conjugated magnetic beads for RNA extraction. *Chem. Asian J.* 12, 1883–1888.
- Priye, A., Wong, S., Bi, Y., Carpio, M., Chang, J., Coen, M., Cope, D., Harris, J., Johnson, J., Keller, A., Lim, R., Lu, S., Millard, A., Pangelinan, A., Pate, N., Smith, L., Chan, K., Ugaz, V.M., 2016. Lab-on-a-drone: toward pinpoint deployment of smartphone-enabled nucleic acid-based diagnostics for mobile health care. *Anal. Chem.* 88, 4651–4660.
- Qiu, X., Zhang, S., Xiang, F., Wu, D., Guo, M., Ge, S., Li, K., Ye, X., Xia, N., Qian, S., 2017a. Instrument-free point-of-care molecular diagnosis of H1N1 based on microfluidic convective PCR. *Sensor. Actuator. B* 243, 738–744.
- Qiu, Z., Shu, J., He, Y., Lin, Z., Zhang, K., Lv, S., Tang, D., 2017b. CdTe/CdSe quantum dot-based fluorescent aptasensor with hemin/G-quadruplex DNzyme for sensitive detection of lysozyme using rolling circle amplification and strand hybridization. *Biosens. Bioelectron.* 87, 18–24.
- Qiu, Z., Shu, J., Tang, D., 2018a. NaYF<sub>4</sub>:Yb,Er upconversion nanotransducer with in situ fabrication of Ag<sub>2</sub>S for near-infrared light responsive photoelectrochemical biosensor. *Anal. Chem.* 90, 12214–12220.
- Qiu, Z., Shu, J., Tang, D., 2018b. Near-infrared-to-ultraviolet light-mediated photoelectrochemical aptasensing platform for cancer biomarker based on core-shell NaYF<sub>4</sub>:Yb,Tm@TiO<sub>2</sub> upconversion microrods. *Anal. Chem.* 90, 1021–1028.
- Roche, P.J.R., Najih, M., Lee, S.S., Beitel, L.K., Carnevale, M.L., Paliouras, M., Kirk, A.G., Trifiroac, M.A., 2017. Real time plasmonic qPCR: how fast is ultra-fast? 30 cycles in 54 seconds. *Analyst* 142, 1746–1755.
- Rodríguez-Enríquez, S., Pacheco-Velázquez, S.C., Gallardo-Pérez, J.C., Marín-Hernández, A., Aguilar-Ponce, J.L., Ruiz-García, E., Ruiz-Godoy-Rivera, L.M., Meneses-García, A., Moreno-Sánchez, R., 2011. Multi-biomarker pattern for tumor identification and prognosis. *J. Cell. Biochem.* 112, 2703–2715.
- Roy, P., Anand, N.K., Banerjee, D., 2013. A review of flow and heat transfer in rotating microchannels. *Procedia Eng* 56, 7–17.
- Saiki, R.K., Scharf, S., Faloona, F., Mullis, K.B., Horn, G.T., Erlich, H.A., Arnheim, N., 1985. Enzymatic amplification of beta-globin genomic sequences and restriction site analysis for diagnosis of sickle cell anemia. *Science* 230, 1350–1354.
- Saiki, R.K., Bugawan, T.L., Horn, G.T., Mullis, K.B., Erlich, H.A., 1986. Analysis of enzymatically amplified  $\beta$ -globin and HLA-DQ $\alpha$  DNA with allele-specific oligonucleotide probes. *Nature* 324, 163–166.
- Saiki, A.K., Gelfand, D.H., Stoffel, S., Scharf, S.J., Higuchi, R., Horn, G.T., Mullis, K.B., Erlich, H.A., 1988a. Primer-directed enzymatic amplification of DNA with a thermostable DNA polymerase. *Science* 239, 487–491.
- Saiki, R.K., Gelfand, D.H., Stoffel, S., Scharf, S.J., Higuchi, R., Horn, G.T., Mullis, K.B., Erlich, H.A., 1988b. Primer-Directed enzymatic amplification of DNA with a thermostable DNA polymerase. *Science* 239, 487–491.
- Schrader, C., Schielke, A., Ellerbroek, L., John, R., 2012. PCR inhibitors – occurrence, properties and removal. *J. Appl. Microbiol.* 113, 1014–1026.
- Schweitzer, B., Roberts, S., Grimwade, B., Shao, W., Wang, M., Fu, Q., Shu, Q., Laroche, I., Zhou, Z., Tchernev, V.T., Christiansen, J., Velleca, M., Kingsmore, S.F., 2002. Multiplexed protein profiling on microarrays by rolling-circle amplification. *Nat. Biotechnol.* 20, 359–365.
- Semper, A.E., Broadhurst, M.J., Richards, J., Foster, G.M., Simpson, A.J.H., Logue, C.H., Kelly, J.D., Miller, A., Brooks, T.J.G., Murray, M., Pollock, N.R., 2016. Performance of the GeneXpert ebola assay for diagnosis of ebola virus disease in Sierra Leone: a field evaluation study. *PLoS Med.* 13, e1001980.
- Shaw, K.J., Docker, P.T., Yelland, J.V., Dyer, C.E., Greenman, J., Greenway, G.M., Haswell, S.J., 2010. Rapid PCR amplification using a microfluidic device with integrated microwave heating and air impingement cooling. *Lab Chip* 10, 1725–1728.
- Shen, C., Yang, W., Ji, Q., Maki, H., Dong, A., Zhang, Z., 2009. NanoPCR observation: different levels of DNA replication fidelity in nanoparticle-enhanced polymerase chain reactions. *Nanotechnology* 20, 455103.
- Sherafat, M., 2018. Tree-based machine learning algorithms identified minimal set of miRNA biomarkers for breast cancer diagnosis and molecular subtyping. *Gene* 677, 111–118.
- Shu, B., Zhang, C., Xing, D., A sample-to-answer, real-time convective polymerase chain reaction system for point-of-care diagnostics. *Biosens. Bioelectron.* 97, 360–368.
- Shu, B., Zhang, C., Xing, D., 2017. A sample-to-answer, real-time convective polymerase chain reaction system for point-of-care diagnostics. *Biosens. Bioelectron.* 97, 360–368.
- Sidstedt, M., Hedman, J., Romsos, E.L., Waitara, L., Wadsö, L., Steffen, C.R., Vallone, P.M., Rådström, P., 2018. Inhibition mechanisms of hemoglobin, immunoglobulin G, and whole blood in digital and real-time PCR. *Anal. Bioanal. Chem.* 410, 2569–2583.
- Siravegna, G., Marsoni, S., Siena, S., Bardelli, A., 2017. Integrating liquid biopsies into the management of cancer. *Nat. Rev. Clin. Oncol.* 14, 531–548.
- Snodgrass, R., Gardner, A., Semeere, A., Koppa, V.L., Duru, J., Maurer, T., Martin, J., Cesarman, E., Erickson, D., 2018. A portable device for nucleic acid quantification powered by sunlight, a flame or electricity. *Nat. Biomed. Eng.* 2, 657–665.
- Solinas, A., Brown, L.J., McKeen, C., Mellor, J.M., Nicol, J., Thelwell, N., Brown, T., 2001. Duplex Scorpion primers in SNP analysis and FRET applications. *Nucleic Acids Res.* 29, e96.
- Son, J.H., Cho, B., Hong, S., Lee, S.H., Hoxha, O., Haack, A.J., Lee, L.P., 2015. Ultrafast photonic PCR. *Light Sci. Appl.* 4, e280.
- Starr, C.R., Villazana, E.T., Chapleau, R.R., Masserang, D.L., 2015. Optimizing the Roche LightCycler for single-tube multiplexed RT-PCR assays. *J. Clin. Diagn. Res.* 9, DM01–DM03.
- Systems, B.M. Australia. <https://biomolecularsystems.com/>.
- Szuhai, K., Ouweland, J.M.v.d., Dirks, R.W., Lemaître, M., Truffert, J.-C., Janssen, G.M., Tanke, H.J., Holme, E., Maassen, A., Raapa, A.K., 2001. Simultaneous A8344G heteroplasmic and mitochondrial DNA copy number quantification in myoclonus epilepsy and ragged-red fibers (MERRF) syndrome by a multiplex molecular beacon based real-time fluorescence PCR. *Nucleic Acids Res.* 29, e13.
- Tachibana, H., Saito, M., Shibuya, S., Tsuji, K., Miyagawa, N., Yamanaka, K., EiichiTamiy, 2015. On-chip quantitative detection of pathogen genes by autonomous microfluidic PCR platform. *Biosens. Bioelectron.* 74, 725–730.
- Tindall, K.R., Kunkel, T.A., 1988. Fidelity of DNA synthesis by the *Thermus aquaticus* DNA polymerase. *Biochemistry* 27, 6008–6013.
- Tomita, N., Mori, Y., Kanda, H., Notomi, T., 2008. Loop-mediated isothermal amplification (LAMP) of gene sequences and simple visual detection of products. *Nat. Protoc.* 3, 877–882.
- Troger, V., Niemann, K., Gartig, C., Kuhlmeier, D., 2015. Isothermal amplification and quantification of nucleic acids and its use in microsystems. *J. Nanomed. Nanotechnol.* 6, 282.
- Tsaloglou, M.-N., Watson, R.J., Rushworth, C.M., Zhao, Y., Niu, X., Sutton, J.M., Morganc, H., Real-time microfluidic recombinase polymerase amplification for the toxin B gene of *Clostridium difficile* on a SlipChip platform. *Analyst* 140, 258–264.
- Tyagi, S., Kramer, F.R., 1996. Molecular beacons: probes that fluoresce upon hybridization. *Nat. Biotechnol.* 14, 303–308.
- Tyagi, S., Bratu, D.P., Kramer, F.R., 1998. Multicolor molecular beacons for allele discrimination. *Nat. Biotechnol.* 1998, 49–53.
- Tyagi, S., Marras, S.A.E., Kramer, F.R., 2000. Wavelength-shifting molecular beacons. *Nat. Biotechnol.* 18, 1191–1196.
- Ugaz, V.M., Krishnan, M., 2004. Novel convective flow based approaches for high-throughput PCR thermocycling. *J. Assoc. Lab. Autom.* 9, 318–323.
- Ullrich, L., Campbell, S., Krieg-Schneider, F., Bursgens, F., Stehr, J., 2017. Ultra-fast PCR technologies for point-of-care testing. *J. Lab. Med.* 41, 239–244.
- Vet, J.A.M., Majithia, A.R., Marras, S.A.E., Tyagi, S., Dube, S., Poesz, B.J., Kramer, F.R., 1999. Multiplex detection of four pathogenic retroviruses using molecular beacons. *Proc. Natl. Acad. Sci.* 96, 6394–6399.
- Walker, G.T., Fraiser, M.S., Schram, J.L., Little, M.C., Nadeau, J.G., Malinowski, D.P., 1992. Strand displacement amplification—an isothermal, in vitro DNA amplification technique. *Nucleic Acids Res.* 20, 1691–1696.
- Waltz, E., 2017. After theranos. *Nat. Biotechnol.* 35, 11–15.
- Wang, D., Khosla, A., Gargya, R., Irshad, H., Beck, A.H., 2016. Deep Learning for Identifying Metastatic Breast Cancer. *arXiv* 1606.05718.
- Webb, J.A., Bardhan, R., 2014. Emerging advances in nanomedicine with engineered gold nanostructures. *Nanoscale* 6, 2502–2530.
- Wei, Q., Qi, H., Luo, W., Tseng, D., Ki, S.J., Wan, Z., Göröcs, Z., Bentolila, L.A., Wu, T.-T., Sun, R., Ozcan, A., 2013. Fluorescent imaging of single nanoparticles and viruses on a smartphone. *ACS Nano* 7, 9147–9155.
- Whitcombe, D., Theaker, J., Guy, S.P., Brown, T., Little, S., 1999. Detection of PCR products using self-probing amplicons and fluorescence. *Nat. Biotechnol.* 17, 804–807.
- Wittwer, C.T., Fillmore, G.C., Hillyard, D.R., 1989. Automated polymerase chain reaction in capillary tubes with hot air. *Nucleic Acids Res.* 17, 4353–4357.
- Yager, P., Edwards, T., Fu, E., Helton, K., Nelson, K., Tam, M.R., Weigl, B.H., 2006. Microfluidic diagnostic technologies for global public health. *Nature* 442, 412–418.
- Yang, W., Mi, L., Cao, X., Zhang, X., Fan, C., Hu, J., 2008. Evaluation of gold nanoparticles as the additive in real-time polymerase chain reaction with SYBR Green I dye. *Nanotechnology* 19, 255101.
- Yeh, E.-C., Fu, C.-C., Hu, L., Thakur, R., Feng, J., Lee, L.P., 2017. Self-powered integrated microfluidic point-of-care low-cost enabling (SIMPLE) chip. *Sci. Adv.* 3, e1501645.
- Yu, Y., Li, B., Baker, C.A., Zhang, X., Roper, M.G., 2012. Quantitative polymerase chain reaction using infrared heating on a microfluidic chip. *Anal. Chem.* 84, 2825–2829.
- Yuan, Y., Shi, Y., Li, C., Kim, J., Cai, W., Han, Z., Feng, D.D., 2016. DeepGene: an advanced cancer type classifier based on deep learning and somatic point mutations. *BMC Bioinf.* 17, 476.
- Yuce, M., Kurt, H., Mokkapatia, V.R.S.S., Budak, H., 2014. Employment of nanomaterials in polymerase chain reaction: insight into the impacts and putative operating mechanisms of nano-additives in PCR. *RSC Adv.* 4, 36800.
- Zeng, R., Luo, Z., Zhang, L., Tang, D., 2018a. Platinum nanozyme-catalyzed gas generation for pressure-based bioassay using polyaniline nanowires-functionalized graphene oxide framework. *Anal. Chem.* 90, 12299–12306.
- Zeng, R., Su, L., Luo, Z., Zhang, L., Lu, M., Tang, D., 2018b. Ultrasensitive and label-free electrochemical aptasensor of kanamycin coupling with hybridization chain reaction and strand-displacement amplification. *Anal. Chim. Acta* 1038, 21–28.
- Zeng, R., Luo, Z., Su, L., Zhang, L., Tang, D., Niessner, R., Knopp, D., 2019a. Palindromic molecular beacon based ZScheme BiOCl-Au-CdS photoelectrochemical biodection. *Anal. Chem.* 91, 2447–2454.
- Zeng, R., Zhang, L., Su, L., Luo, Z., Zhou, Q., Tang, D., 2019b. Photoelectrochemical bioanalysis of antibiotics on rGO-Bi<sub>2</sub>WO<sub>6</sub>-Au based on branched hybridization chain reaction. *Biosens. Bioelectron.* 133, 100–106.
- Zeschknig, M., Bohringer, S., Price, E.A., Onadim, Z., Maßhofer, L., Lohmann, D.R., 2004. A novel real-time PCR assay for quantitative analysis of methylated alleles (QAMA): analysis of the retinoblastoma locus. *Nucleic Acids Res.* 32, e125.
- Zhang, B., Liu, B., Tang, D., Niessner, R., Chen, G., Knopp, D., 2012. DNA-based hybridization chain reaction for amplified bioelectronic signal and ultrasensitive detection of proteins. *Anal. Chem.* 84, 5392–5399.
- Zhang, K., Lv, S., Lin, Z., Tang, D., 2017. CdS:Mn quantum dot-functionalized g-C<sub>3</sub>N<sub>4</sub> nanohybrids as signal-generation tags for photoelectrochemical immunoassay of



- prostate specific antigen coupling DNAzyme concatamer with enzymatic biocatalytic precipitation. *Biosens. Bioelectron.* 95, 34–40.
- Zhang, K., Lv, S., Lin, Z., Li, M., Tang, D., 2018a. Bio-bar-code-based photoelectrochemical immunoassay for sensitive detection of prostate-specific antigen using rolling circle amplification and enzymatic biocatalytic precipitation. *Biosens. Bioelectron.* 15, 159–166.
- Zhang, K., Lv, S., Lu, M., Tang, D., 2018b. Photoelectrochemical biosensing of disease marker on p-type Cu-doped Zn<sub>0.3</sub>Cd<sub>0.7</sub>S based on RCA and exonuclease III amplification. *Biosens. Bioelectron.* 117, 590–596.
- Zhou, Q., Lin, Y., Zhang, K., Li, M., Tang, D., 2018. Reduced graphene oxide/BiFeO<sub>3</sub> nanohybrids-based signal-on photoelectrochemical sensing system for prostate-specific antigen detection coupling with magnetic microfluidic device. *Biosens. Bioelectron.* 101, 146–152.